Conflicting results have been reported as to whether genetic variations (Val66Met and C270T) of the brain-derived neurotrophic factor gene (BDNF) confer susceptibility to Alzheimer's disease (AD). We genotyped these polymorphisms in a Japanese sample of 657 patients with AD and 525 controls, and obtained weak evidence of association for Val66Met ($P = 0.063$), but not for C270T. After stratification by sex, we found a significant allelic association between Val66Met and AD in women ($P = 0.017$), but not in men. To confirm these observations, we collected genotyping data for each sex from 16 research centers worldwide (4,711 patients and 4,537 controls in total). The meta-analysis revealed that there was a clear sex difference in the allelic association; the Met66 allele confers susceptibility to AD in women (odds ratio = 1.14, 95% CI 1.05–1.24, $P = 0.002$), but not in men. Our results provide evidence that the Met66 allele of BDNF has a sexually dimorphic effect on susceptibility to AD.

Key words: Alzheimer's disease (AD); brain-derived neurotrophic factor (BDNF); meta-analysis; polymorphism; sex difference

INTRODUCTION

Alzheimer's disease (AD) is a common neurodegenerative disease and is neuropathologically characterized by loss and atrophy of basal forebrain cholinergic neurons and the limbic structures [Mattson, 2004]. Mutations in several genes are known to cause familial AD, namely those encoding amyloid precursor protein [Goate et al., 1991], presenilin-1 [Sherrington et al., 1995], and presenilin-2 [Levy-Lahad et al., 1995]. The ε4 allele of the apolipoprotein E (*APOE*) gene confers susceptibility to familial and sporadic AD [Saunders et al., 1993]. However, AD is a genetically complex disorder and these genetic markers for AD cannot explain the overall genetic susceptibility. Thus, additional genes may be involved in the development of AD.

Since neurotrophins such as nerve growth factor (NGF), brain-derived neurotrophic factor (BDNF), and neurotrophin-3 (NT-3) promote the development, regeneration, survival, and maintenance of function of neurons [Reichardt, 2006], polymorphisms of the genes encoding these proteins may confer susceptibility to neurodegenerative diseases. Several lines of evidence have suggested that *BDNF*, in particular, is an important candidate gene for susceptibility to AD. Reduced *BDNF* mRNA levels were observed in postmortem hippocampi and temporal cortices of patients with AD [Connor et al., 1997], and lower protein levels of BDNF in the entorhinal cortex were reported in AD [Hock et al., 2000]. Immunohistochemical and Western blotting studies revealed a selective decline of the BDNF/TrkB neurotrophic signaling pathway in the frontal cortex and hippocampus in AD [Ferrer et al., 1999].

Based on these observations, a number of genetic association studies have been performed for two polymorphisms of *BDNF*, Val66Met, and C270T. The non-synonymous polymorphism, Val66Met, is a functional single-nucleotide polymorphism (SNP), G to A substitution at nucleotide 196, which results in the Val66-to-Met amino acid change in the 5′ pro-region of the human BDNF protein [Ventriglia et al., 2002]. Two studies reported that the Met66 allele was significantly associated with an increased risk of AD [Saarela et al., 2006; Tsai et al., 2006], while one study reported that the Val66 allele was the risk-increasing allele [Matsushita et al., 2005]. The majority of studies, however, have found no significant association (Supplementary Fig. 1) [Ventriglia et al., 2002; Bagnoli et al., 2004; Combarros et al., 2004; Nacmias et al., 2004; Bian et al., 2005; Bodner et al., 2005; Desai et al., 2005; Lee et al., 2005; Li et al., 2005; Nishimura et al., 2005; Vepsalainen et al., 2005; Akatsu et al., 2006; Forero et al., 2006; Zhang et al., 2006; He et al., 2007; Huang et al., 2007]. The C270T polymorphism in the non-coding region of *BDNF* was detected by our group and found to be associated with late-onset AD [Kunugi et al., 2001]. Subsequently, two other groups reported that the T270 allele was significantly associated with an increased risk of AD [Nishimura et al., 2004; Olin et al., 2005], while one group reported the opposite [Saarela et al., 2006]. Other studies reported no significant association (Supplementary Fig. 2) [Riemenschneider et al., 2002; Bagnoli et al., 2004; Nishimura et al., 2004; Bodner et al., 2005; Desai et al., 2005; Lee et al., 2005; Matsushita et al., 2005; Akatsu et al., 2006; Tsai et al., 2006; Zhang et al., 2006; Huang et al., 2007]. These conflicting results require further investigation.

METHODS

Case–Control Study Sample

We genotyped 657 patients with AD (427 females; 73.5 years [SD] 8.7) and 525 healthy controls (305 females; 67.1 years [SD] 10.3) who were recruited around the Tokyo Metropolitan area, Japan. Diagnoses were made by neurologists according to the National Institute of Neurological and Communicative Diseases and Stroke/Alzheimer's Disease and Related Disorders Association (NINCDS-ADRDA) criteria [McKhann et al., 1984] for "probable AD." The numbers of individuals with and without a family history of dementia were 211 and 425, respectively, while the remaining 21 individuals had undetermined family histories. Controls were interviewed and those who had a family history of dementia within their first-degree relatives were not enrolled in the study. All subjects were biologically unrelated Japanese individuals. After description of the study, written informed consent was obtained from every subject. The study protocol was approved from the ethics committee of the National Center of Neurology and Psychiatry, Japan.

Genotyping

The two SNPs of *BDNF* were genotyped using the TaqMan 5′-exonuclease allelic discrimination assay. TaqMan probes of the "Assay-On-Demand" (C__11592758_10) for Val66Met (rs6265) and TaqMan primers (forward: GGAGCCAGAATCGGAACCA; reverse: CCAGCGCTTGCCTACCT) and probes (VIC: CTCACGGGTCCCCG; FAM: CTCACGAGTCCCCG) of the "Assay-by-Design" for C270T and Universal PCR Master Mix were obtained from Applied Biosystems (Foster City, CA). Thermal cycling conditions for the polymerase chain reaction (PCR) were one cycle at 95°C for 10 min followed by 40 cycles of 95°C for 15 sec and 58°C for 1 min. After amplification, the allele-specific fluorescence was measured on ABI PRISM 7900 Sequence Detection

System (Applied Biosystems). Genotype data were read blind to the case–control status. We also genotyped the subjects for the *APOE* gene, according to the methods of Wenham et al. [1991].

Meta-Analysis

To examine whether there was a possible sex difference in the effect of these polymorphisms on AD in a larger sample, we organized a multi-center collaborative study and performed a meta -analysis. We searched for published case–control association studies of the Val66Met or C270T polymorphism with AD in the PubMed database (National Center for Biotechnology Information; NCBI; www.ncbi.nlm.nih.gov/), using combinations of terms "BDNF," "brain-derived neurotrophic factor," "polymorphism," "Val66Met," "C270T," "C-270T," and "Alzheimer." Additionally, reference lists of these and relevant articles, and the AlzGene Database (www.alzforum.org/) [Bertram et al., 2007] were referred to. As a result, 23 association studies of AD with Val66Met (Supplementary Table III) and 18 with C270T (Supplementary Table IV) were identified. Then an e-mail calling for participation in the collaborative study was sent to corresponding and first authors. Sixteen research groups for the Val66Met and 12 for the C270T responded and participated in this study. Genotype data with information on sex were combined.

Genotypes in the control groups from all research groups were in Hardy–Weinberg equilibrium. In the meta-analysis, heterogeneity, publication bias, sensitivity analysis, and Rosenthal's failsafe N were determined. Meta-analytic procedures were carried out using Comprehensive Meta-Analysis v.2.0 (Biostat, Inc., Englewood, NJ). To confirm that there was no significant difference in the allele distributions of patients and controls between the collected and the uncollected data (i.e., studies whose authors did not respond to us), Breslow–Day tests were performed using R software (R Development Core Team, 2007). With respect to Val66Met, the summary data for the Breslow–Day tests are shown in Supplementary Table V. There was no significant difference between the collected and uncollected data ($\chi^2 = 2.0$, df = 1, $P = 0.15$).

RESULTS

Case–Control Study

Genotype distributions for Val66Met, C270T, and *APOE* were in Hardy–Weinberg equilibrium for both patients and controls (data not shown). Genotype distributions for *APOE* were significantly different between the patients and controls as expected ($P = 2 \times 10^{-18}$) (Supplementary Table I). Genotype and allele distributions for Val66Met are shown in Table I. There was a trend towards an increased frequency of the Met66 allele in patients compared to controls ($P = 0.063$). When men and women were examined separately, the allele distribution differed between the two groups in females (odds ratio [OR] = 1.30, 95% CI = 1.05–1.60, $P = 0.017$), but not in males (OR = 1.02, 95% CI = 0.78–1.32, $P = 0.91$) (Table I).

The genotype and allele distributions for C270T are shown in Supplementary Table II. There was no significant difference in the genotype or allele distribution between the patients and controls.

TABLE I. Genotype and Allele Distributions for the Val66Met Polymorphism of BDNF in Patients With Alzheimer's Disease and Controls

	Genotype distribution									Allele distribution					
	Patients				Controls					Patients			Controls		
	n	Val/Val	Val/Met	Met/Met	n	Val/Val	Val/Met	Met/Met	*P*-value, df = 2	Val	Met		Val	Met	*P*-value, df = 1
Total	657	218 (0.33)	319 (0.49)	120 (0.18)	525	197 (0.38)	249 (0.47)	79 (0.15)	0.18 ($\chi^2 = 3.4$)	755 (0.57)	559 (0.53)		643 (0.61)	407 (0.39)	0.063 ($\chi^2 = 3.5$)
Female	427	142 (0.33)	205 (0.48)	80 (0.19)	305	122 (0.40)	143 (0.47)	40 (0.13)	0.057 ($\chi^2 = 5.7$)	489 (0.57)	365 (0.60)		387 (0.63)	223 (0.37)	0.017 ($\chi^2 = 5.7$)
Male	230	76 (0.33)	114 (0.50)	40 (0.17)	220	75 (0.34)	106 (0.48)	39 (0.18)	0.96 ($\chi^2 = 0.09$)	266 (0.58)	194 (0.44)		256 (0.58)	184 (0.42)	0.91 ($\chi^2 = 0.01$)

TABLE II. Genotype and Allele Distributions for the Val66Met Polymorphism of *BDNF* in Female Subjects

		Genotype distribution								Allele distribution			
		Patients				Controls				Patients		Controls	
Study	Ethnicity	n	Val/Val	Val/Met	Met/Met	n	Val/Val	Val/Met	Met/Met	Val	Met	Val	Met
Akatsu et al. [2006]	Asian	58	16	36	6	86	30	42	14	68	48	102	70
Bian et al. [2005]	Asian	108	20	67	21	105	36	47	22	107	109	119	91
He et al. [2007]	Asian	318	92	152	74	332	97	170	65	336	300	364	300
Matsushita et al. [2005]	Asian	340	117	170	53	321	104	154	63	404	276	362	280
Tsai et al. [2006]	Asian	84	19	50	15	101	33	50	18	88	80	116	86
Current study	Asian	427	142	205	80	305	122	143	40	489	365	387	223
Subtotal		1,335	406	680	249	1,250	422	606	222	1,492	1,178	1,450	1,050
Combarros et al. [2004]	Caucasian	161	107	47	7	155	105	44	6	261	61	254	56
Desai et al. [2005]	Caucasian	669	449	201	19	411	287	115	9	1,099	239	689	133
Li et al. [2005] (UCSD)[a]	Caucasian	87	51	32	4	226	150	67	9	134	40	367	85
Li et al. [2005] (WashU)[b]	Caucasian	248	163	81	4	215	150	60	5	407	89	360	70
Li et al. [2005] (UK)[c]	Caucasian	265	178	73	14	270	192	73	5	429	101	457	83
Nacmias et al. [2004]	Caucasian	58	36	19	3	61	39	22	0	91	25	100	22
Saarela et al. [2006]	Caucasian	68	45	21	2	56	46	10	0	111	25	102	10
Subtotal		1,556	1,029	474	53	1,394	969	391	34	2,532	580	2,329	459
Desai et al. [2005]	African-American	46	42	4	0	33	31	2	0	88	4	64	2
Forero et al. [2006]	Mixed	73	51	20	2	115	90	23	2	122	24	203	27
Lee et al. [2005]	Unknown	61	31	28	2	38	20	14	4	90	32	54	22
Total		3,071	1,559	1,206	306	2,830	1,532	1,036	262	4,324	1,818	4,100	1,560

[a]UCSD sample from the University of California, San Diego.
[b]WashU sample from the Washington University.
[c]UK sample from Cardiff University, Wales College of Medicine and King's College London.

TABLE III. Genotype and Allele Distributions for the Val66Met Polymorphism of *BDNF* in Male Subjects

		Genotype distribution								Allele distribution			
		Patients				Controls				Patients		Contorls	
Study	Ethnicity	n	Val/Val	Val/Met	Met/Met	n	Val/Val	Val/Met	Met/Met	Val	Met	Val	Met
Akatsu et al. [2006]	Asian	37	9	22	6	22	5	11	6	40	34	21	23
Bian et al. [2005]	Asian	95	29	46	20	134	37	68	29	104	86	142	126
He et al. [2007]	Asian	195	63	93	39	243	68	115	60	219	171	251	235
Matsushita et al. [2005]	Asian	147	54	77	16	150	46	69	35	185	109	161	139
Tsai et al. [2006]	Asian	91	24	42	25	88	31	45	12	90	92	107	69
Current study	Asian	230	76	114	40	220	75	106	39	266	194	256	184
Subtotal		795	255	394	146	857	262	414	181	904	686	938	776
Combarros et al. [2004]	Caucasian	76	42	31	3	63	38	23	2	115	37	99	27
Desai et al. [2005]	Caucasian	329	216	98	15	260	169	82	9	530	128	420	100
Li et al. [2005] (UCSD)	Caucasian	94	54	38	2	126	81	39	6	146	42	201	51
Li et al. [2005] (WashU)	Caucasian	140	88	45	7	134	87	45	2	221	59	219	49
Li et al. [2005] (UK)	Caucasian	72	46	26	0	89	56	28	5	118	26	140	38
Nacmias et al. [2004]	Caucasian	25	12	10	3	36	16	16	4	34	16	48	24
Saarela et al. [2006]	Caucasian	29	16	13	0	45	35	7	3	45	13	77	13
Subtotal		765	474	261	30	753	482	240	31	1,209	321	1,204	302
Desai et al. [2005]	African-American	18	17	1	0	12	11	1	0	35	1	23	1
Forero et al. [2006]	Mixed	28	21	7	0	53	41	11	1	49	7	93	13
Lee et al. [2005]	Unknown	34	14	19	1	32	12	16	4	47	21	40	24
Total		1,640	781	682	177	1,707	808	682	217	2,244	1,036	2,298	1,116

Also when sexes were examined separately, no significant association was found for either sex.

Meta-Analysis

With respect to Val66Met, individual studies contained 64–998 patients with AD and 45–671 controls, and the combined sample consisted of 4,711 patients and 4,537 controls (Supplementary Table III). There was no heterogeneity across studies (total: $Q = 26.7$, $df = 21$, $P = 0.18$; men: $Q = 16.0$, $df = 15$, $P = 0.38$; women: $Q = 13.5$, $df = 15$, $P = 0.56$). Thus, we performed the fixed effects meta-analyses (Fig. 1, Tables II and III). The meta-analysis showed no significant association between AD and the Met66 allele (OR = 1.05, 95% CI = 0.98–1.11; $Z = 1.43$, $P = 0.15$; Supplementary Fig. 1). Meta-analysis of data in men and women separately revealed a significant association in women (OR = 1.14, 95% CI = 1.05–1.24; $Z = 3.05$, $P = 0.002$; Fig. 1A), but not in men (OR = 0.97, 95% CI = 0.87–1.08; $Z = -0.54$, $P = 0.59$; Fig. 1B). In the sensitivity analysis, the association of the Met66 allele with AD remained significant after removal of any one study (Supplementary Table VI): even if our data were removed, there remained a significant association for women (residual OR = 1.11,

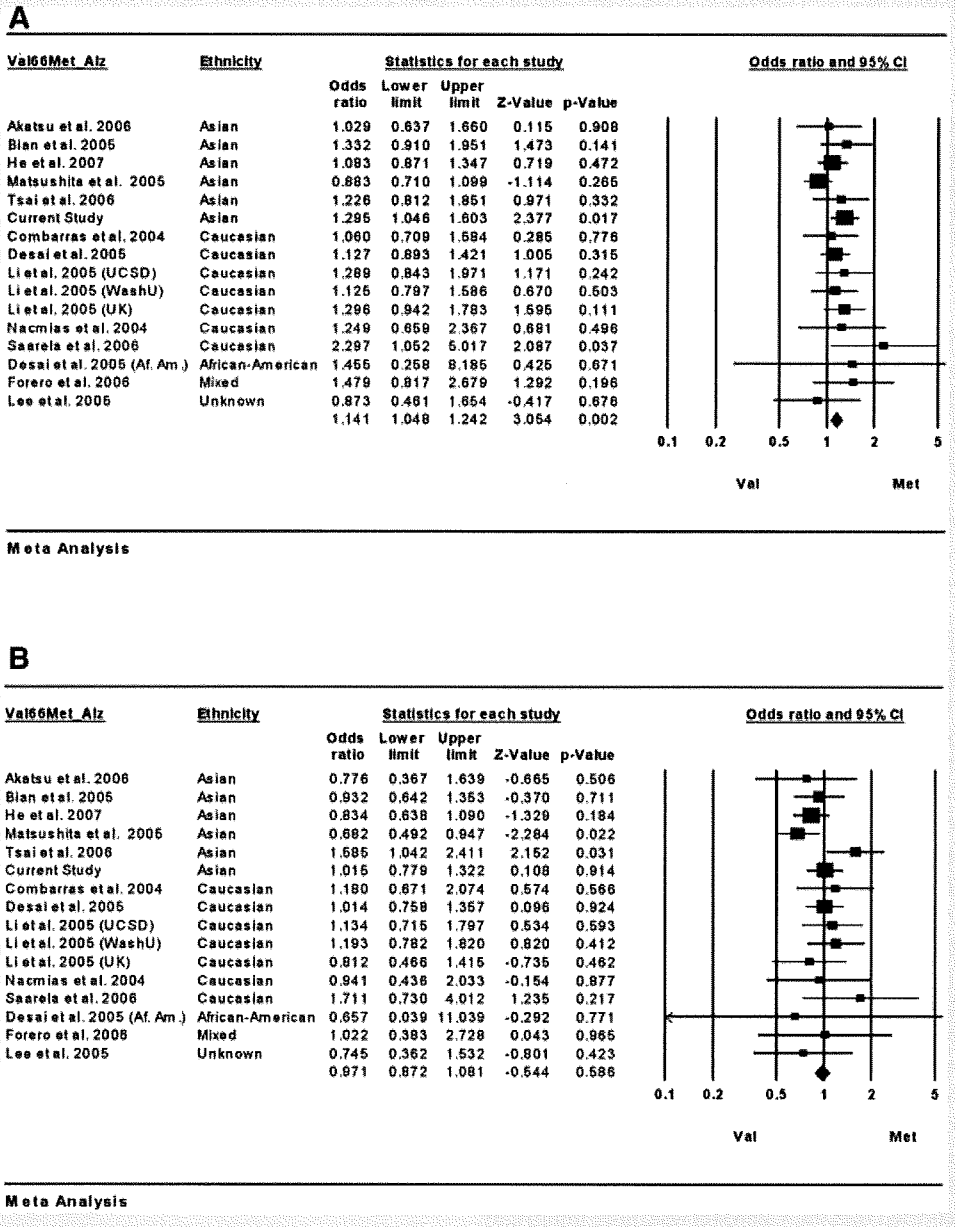

FIG. 1. Forest plots of meta-analysis on the possible association between the Val66Met polymorphism of *BDNF* and Alzheimer's disease in female (A) and male (B) subjects.

95% CI = 1.02–1.22; Z = 2.30, $P = 0.022$). The Rosenthal failsafe N for women was 31 studies. No evidence of publication bias was indicated by Egger's test (intercept = 0.80, 95% CI = −0.37 to 0.54, $t = 1.46$, $P = 0.17$).

Meta-analysis for the C270T polymorphism was performed in the same way. Eighteen studies were identified, of which 12, including ours, participated in the meta-analysis. The individual studies contained 58–722 AD cases and 42–525 controls, and the combined sample consisted of 2,963 subjects with AD and 2,756 controls (Supplementary Tables IV, VII, and VIII). There was a significant heterogeneity between studies (total: Q = 44.7, df = 17, $P < 0.01$; men: Q = 18.8, df = 11, $P = 0.065$; women: Q = 30.2, df = 11, $P < 0.01$). Thus, we performed the random effects meta-analyses (Supplementary Fig. 2). Our meta-analysis did not show significant association of AD with the T270 allele (random-effect pooled OR = 1.07, 95% CI = 0.83–1.39; Z = 0.54, $P = 0.59$; Supplementary Fig. 2A). Also when men and women were examined separately, our meta-analysis revealed no significant association with AD in women (OR = 1.08, 95% CI = 0.70–1.67; Z = 0.37, $P = 0.72$; Supplementary Fig. 2B) or in men (OR = 1.19, 95% CI = 0.77–1.84; Z = 0.78, $P = 0.43$; Supplementary Fig. 2C).

DISCUSSION

We showed, for the first time, a significant allelic association between the Val66Met of *BDNF* and AD in women in our Japanese sample ($P = 0.017$). In contrast, we did not observe such an association in men. When the multi-center study was organized, the sexually dimorphic effect of the Val66Met on the development of AD was similarly observed in the much larger sample (4,711 patients and 4,537 controls) from 16 research centers worldwide. These results provide evidence suggesting that the Met66 allele has a risk-increasing effect on AD in women, but not in men.

The Met66-BDNF protein has been shown to be associated with reduced transport of BDNF from the Golgi region to appropriate secretory granules in neurons, compared with the Val66-BDNF protein [Egan et al., 2003; del Toro et al., 2006]. It is reasonable to assume that the Met66 is associated with lower secretion of BDNF, which could result in attenuation of the survival signal of BDNF, compared with the Val66. In accordance with this, individuals carrying the Met66 allele have been reported to have decreased brain structures (e.g., hippocampus) than those individuals who did not carry the allele [Pezawas et al., 2004; Szeszko et al., 2005; Agartz et al., 2006; Bueller et al., 2006; Ho et al., 2006; Nemoto et al., 2006; Frodl et al., 2007; Liguori et al., 2007]. Of note, we found that female individuals carrying the Met66 allele showed more widespread age-associated volume reduction in the dorsolateral prefrontal cortices than male Met66 carriers [Nemoto et al., 2006].

Several lines of evidence suggest the sexual dimorphic effects of *BDNF*. The study of *BDNF* conditional knockout mice demonstrated sexually dimorphic effects in depression- and anxiety-related behavior [Monteggia et al., 2007]. A recent sexually stratified meta-analysis reported that the Val66Met was more important in the development of major depressive disorder in men than in women [Verhagen et al., 2008]. In Parkinson's disease as well, a sex difference in the effect of *BDNF* was reported [Foltynie et al., 2005]. Many epidemiological studies reported higher prevalence and incidence of AD in women than in men [Fratiglioni et al., 1997]. In an animal model of neurodegenerative diseases, aged female mice were more sensitive to kainic acid-induced excitotoxicity to neurons, compared with aged males [Zhang et al., 2008]. These findings are in line with our observations of the sexually dimorphic effect of *BDNF* on AD. Indeed, estrogen plays an important role in the expression of BDNF. Estrogen receptors co-localize with BDNF-synthesizing neurons in the forebrain [Miranda et al., 1993] and estrogen induces BDNF expression through the estrogen response element [Sohrabji et al., 1995].

With respect to the C270T, we obtained no evidence for an association with AD in our sample alone or in the combined sample. We observed a significant heterogeneity across studies in the meta-analysis. In addition, the allele frequency of the risk allele (T270) reported in the original study [Kunugi et al., 2001] was quite low (0.03 in total), indicating the possibility of type II error due to lack of statistical power. Thus, further studies are required to draw any conclusion.

In conclusion, we provided the first meta-analytic evidence that the Met66 allele of *BDNF* has a sexually dimorphic effect on susceptibility to AD. Studies elucidating the molecular mechanisms underlying this association are warranted.

ACKNOWLEDGMENTS

This study was supported by Health and Labor Sciences Research Grants (Research on Psychiatric and Neurological Diseases and Mental Health), the Program for Promotion of Fundamental Studies, in Health Sciences of the National Institute of Biomedical Innovation (NIBIO), and Grant-in-Aid for Scientific Research from the Japan Society for the Promotion of Science (JSPS).

REFERENCES

Agartz I, Sedvall GC, Terenius L, Kulle B, Frigessi A, Hall H, Jonsson EG. 2006. BDNF gene variants and brain morphology in schizophrenia. Am J Med Genet Part B 141B(5):513–523.

Akatsu H, Yamagata HD, Kawamata J, Kamino K, Takeda M, Yamamoto T, Miki T, Tooyama I, Shimohama S, Kosaka K. 2006. Variations in the BDNF gene in autopsy-confirmed Alzheimer's disease and dementia with Lewy bodies in Japan. Dement Geriatr Cogn Disord 22(3):216–222.

Bagnoli S, Nacmias B, Tedde A, Guarnieri BM, Cellini E, Petruzzi C, Bartoli A, Ortenzi L, Sorbi S. 2004. Brain-derived neurotrophic factor genetic variants are not susceptibility factors to Alzheimer's disease in Italy. Ann Neurol 55(3):447–448.

Bertram L, McQueen MB, Mullin K, Blacker D, Tanzi RE. 2007. Systematic meta-analyses of Alzheimer disease genetic association studies: The AlzGene database. Nat Genet 39(1):17–23.

Bian JT, Zhang JW, Zhang ZX, Zhao HL. 2005. Association analysis of brain-derived neurotrophic factor (BDNF) gene 196 A/G polymorphism with Alzheimer's disease (AD) in mainland Chinese. Neurosci Lett 387(1):11–16.

Bodner SM, Berrettini W, van Deerlin V, Bennett DA, Wilson RS, Trojanowski JQ, Arnold SE. 2005. Genetic variation in the brain derived neurotrophic factor gene in Alzheimer's disease. Am J Med Genet Part B 134B(1):1–5.

Bueller JA, Aftab M, Sen S, Gomez-Hassan D, Burmeister M, Zubieta JK. 2006. BDNF Val66Met allele is associated with reduced hippocampal volume in healthy subjects. Biol Psychiatry 59(9):812–815.

Combarros O, Infante J, Llorca J, Berciano J. 2004. Polymorphism at codon 66 of the brain-derived neurotrophic factor gene is not associated with sporadic Alzheimer's disease. Dement Geriatr Cogn Disord 18(1):55–58.

Connor B, Young D, Yan Q, Faull RL, Synek B, Dragunow M. 1997. Brain-derived neurotrophic factor is reduced in Alzheimer's disease. Brain Res Mol Brain Res 49(1–2):71–81.

del Toro D, Canals JM, Gines S, Kojima M, Egea G, Alberch J. 2006. Mutant huntingtin impairs the post-Golgi trafficking of brain-derived neurotrophic factor but not its Val66Met polymorphism. J Neurosci 26(49): 12748–12757.

Desai P, Nebes R, DeKosky ST, Kamboh MI. 2005. Investigation of the effect of brain-derived neurotrophic factor (BDNF) polymorphisms on the risk of late-onset Alzheimer's disease (AD) and quantitative measures of AD progression. Neurosci Lett 379(3):229–234.

Egan MF, Kojima M, Callicott JH, Goldberg TE, Kolachana BS, Bertolino A, Zaitsev E, Gold B, Goldman D, Dean M, et al. 2003. The BDNF val66met polymorphism affects activity-dependent secretion of BDNF and human memory and hippocampal function. Cell 112(2):257–269.

Ferrer I, Marin C, Rey MJ, Ribalta T, Goutan E, Blanco R, Tolosa E, Marti E. 1999. BDNF and full-length and truncated TrkB expression in Alzheimer disease. Implications in therapeutic strategies. J Neuropathol Exp Neurol 58(7):729–739.

Foltynie T, Lewis SG, Goldberg TE, Blackwell AD, Kolachana BS, Weinberger DR, Robbins TW, Barker RA. 2005. The BDNF Val66Met polymorphism has a gender specific influence on planning ability in Parkinson's disease. J Neurol 252(7):833–838.

Forero DA, Benitez B, Arboleda G, Yunis JJ, Pardo R, Arboleda H. 2006. Analysis of functional polymorphisms in three synaptic plasticity-related genes (BDNF, COMT AND UCHL1) in Alzheimer's disease in Colombia. Neurosci Res 55(3):334–341.

Fratiglioni L, Viitanen M, von Strauss E, Tontodonati V, Herlitz A, Winblad B. 1997. Very old women at highest risk of dementia and Alzheimer's disease: Incidence data from the Kungsholmen Project, Stockholm. Neurology 48(1):132–138.

Frodl T, Schule C, Schmitt G, Born C, Baghai T, Zill P, Bottlender R, Rupprecht R, Bondy B, Reiser M, et al. 2007. Association of the brain-derived neurotrophic factor Val66Met polymorphism with reduced hippocampal volumes in major depression. Arch Gen Psychiatry 64(4):410–416.

Goate A, Chartier-Harlin MC, Mullan M, Brown J, Crawford F, Fidani L, Giuffra L, Haynes A, Irving N, James L, et al. 1991. Segregation of a missense mutation in the amyloid precursor protein gene with familial Alzheimer's disease. Nature 349(6311):704–706.

He XM, Zhang ZX, Zhang JW, Zhou YT, Tang MN, Wu CB, Hong Z. 2007. Lack of association between the BDNF gene Val66Met polymorphism and Alzheimer disease in a Chinese Han population. Neuropsychobiology 55(3–4):151–155.

Ho BC, Milev P, O'Leary DS, Librant A, Andreasen NC, Wassink TH. 2006. Cognitive and magnetic resonance imaging brain morphometric correlates of brain-derived neurotrophic factor Val66Met gene polymorphism in patients with schizophrenia and healthy volunteers. Arch Gen Psychiatry 63(7):731–740.

Hock C, Heese K, Hulette C, Rosenberg C, Otten U. 2000. Region-specific neurotrophin imbalances in Alzheimer disease: Decreased levels of brain-derived neurotrophic factor and increased levels of nerve growth factor in hippocampus and cortical areas. Arch Neurol 57(6):846–851.

Huang R, Huang J, Cathcart H, Smith S, Poduslo SE. 2007. Genetic variants in brain-derived neurotrophic factor associated with Alzheimer's disease. J Med Genet 44(2):e66.

Kunugi H, Ueki A, Otsuka M, Isse K, Hirasawa H, Kato N, Nabika T, Kobayashi S, Nanko S. 2001. A novel polymorphism of the brain-derived neurotrophic factor (BDNF) gene associated with late-onset Alzheimer's disease. Mol Psychiatry 6(1):83–86.

Lee J, Fukumoto H, Orne J, Klucken J, Raju S, Vanderburg CR, Irizarry MC, Hyman BT, Ingelsson M. 2005. Decreased levels of BDNF protein in Alzheimer temporal cortex are independent of BDNF polymorphisms. Exp Neurol 194(1):91–96.

Levy-Lahad E, Wasco W, Poorkaj P, Romano DM, Oshima J, Pettingell WH, Yu CE, Jondro PD, Schmidt SD, Wang K, et al. 1995. Candidate gene for the chromosome 1 familial Alzheimer's disease locus. Science 269(5226):973–977.

Li Y, Rowland C, Tacey K, Catanese J, Sninsky J, Hardy J, Powell J, Lovestone S, Morris JC, Thal L, et al. 2005. The BDNF Val66Met polymorphism is not associated with late onset Alzheimer's disease in three case-control samples. Mol Psychiatry 10(9):809–810.

Liguori M, Fera F, Gioia MC, Valentino P, Manna I, Condino F, Cerasa A, La Russa A, Clodomiro A, Paolillo A, et al. 2007. Investigating the role of brain-derived neurotrophic factor in relapsing-remitting multiple sclerosis. Genes Brain Behav 6(2):177–183.

Matsushita S, Arai H, Matsui T, Yuzuriha T, Urakami K, Masaki T, Higuchi S. 2005. Brain-derived neurotrophic factor gene polymorphisms and Alzheimer's disease. J Neural Transm 112(5):703–711.

Mattson MP. 2004. Pathways towards and away from Alzheimer's disease. Nature 430(7000):631–639.

McKhann G, Drachman D, Folstein M, Katzman R, Price D, Stadlan EM. 1984. Clinical diagnosis of Alzheimer's disease: Report of the NINCDS-ADRDA Work Group under the auspices of Department of Health and Human Services Task Force on Alzheimer's Disease. Neurology 34(7): 939–944.

Miranda RC, Sohrabji F, Toran-Allerand CD. 1993. Neuronal colocalization of mRNAs for neurotrophins and their receptors in the developing central nervous system suggests a potential for autocrine interactions. Proc Natl Acad Sci USA 90(14):6439–6443.

Monteggia LM, Luikart B, Barrot M, Theobold D, Malkovska I, Nef S, Parada LF, Nestler EJ. 2007. Brain-derived neurotrophic factor conditional knockouts show gender differences in depression-related behaviors. Biol Psychiatry 61(2):187–197.

Nacmias B, Piccini C, Bagnoli S, Tedde A, Cellini E, Bracco L, Sorbi S. 2004. Brain-derived neurotrophic factor, apolipoprotein E genetic variants and cognitive performance in Alzheimer's disease. Neurosci Lett 367(3): 379–383.

Nemoto K, Ohnishi T, Mori T, Moriguchi Y, Hashimoto R, Asada T, Kunugi H. 2006. The Val66Met polymorphism of the brain-derived neurotrophic factor gene affects age-related brain morphology. Neurosci Lett 397(1–2):25–29.

Nishimura AL, Oliveira JR, Mitne-Neto M, Guindalini C, Nitrini R, Bahia VS, de Brito-Marques PR, Otto PA, Zatz M. 2004. Lack of association between the brain-derived neurotrophin factor (C-270T) polymorphism and late-onset Alzheimer's disease (LOAD) in Brazilian patients. J Mol Neurosci 22(3):257–260.

Nishimura M, Kuno S, Kaji R, Kawakami H. 2005. Brain-derived neurotrophic factor gene polymorphisms in Japanese patients with sporadic Alzheimer's disease, Parkinson's disease, and multiple system atrophy. Mov Disord 20(8):1031–1033.

Olin D, MacMurray J, Comings DE. 2005. Risk of late-onset Alzheimer's disease associated with BDNF C270T polymorphism. Neurosci Lett 381(3):275–278.

Pezawas L, Verchinski BA, Mattay VS, Callicott JH, Kolachana BS, Straub RE, Egan MF, Meyer-Lindenberg A, Weinberger DR. 2004. The brain-derived neurotrophic factor val66met polymorphism and variation in human cortical morphology. J Neurosci 24(45):10099–11102.

Reichardt LF. 2006. Neurotrophin-regulated signalling pathways. Philos Trans R Soc Lond B Biol Sci 361(1473):1545–1564.

Riemenschneider M, Schwarz S, Wagenpfeil S, Diehl J, Muller U, Forstl H, Kurz A. 2002. A polymorphism of the brain-derived neurotrophic factor (BDNF) is associated with Alzheimer's disease in patients lacking the Apolipoprotein E epsilon4 allele. Mol Psychiatry 7(7):782–785.

Saarela MS, Lehtimaki T, Rinne JO, Huhtala H, Rontu R, Hervonen A, Roytta M, Ahonen JP, Mattila KM. 2006. No association between the brain-derived neurotrophic factor 196 G>A or 270 C>T polymorphisms and Alzheimer's or Parkinson's disease. Folia Neuropathol 44(1):12–16.

Saunders AM, Strittmatter WJ, Schmechel D, George-Hyslop PH, Pericak-Vance MA, Joo SH, Rosi BL, Gusella JF, Crapper-MacLachlan DR, Alberts MJ, et al. 1993. Association of apolipoprotein E allele epsilon 4 with late-onset familial and sporadic Alzheimer's disease. Neurology 43(8):1467–1472.

Sherrington R, Rogaev EI, Liang Y, Rogaeva EA, Levesque G, Ikeda M, Chi H, Lin C, Li G, Holman K, et al. 1995. Cloning of a gene bearing missense mutations in early-onset familial Alzheimer's disease. Nature 375(6534):754–760.

Sohrabji F, Miranda RC, Toran-Allerand CD. 1995. Identification of a putative estrogen response element in the gene encoding brain-derived neurotrophic factor. Proc Natl Acad Sci USA 92(24):11110–11114.

Szeszko PR, Lipsky R, Mentschel C, Robinson D, Gunduz-Bruce H, Sevy S, Ashtari M, Napolitano B, Bilder RM, Kane JM, et al. 2005. Brain-derived neurotrophic factor val66met polymorphism and volume of the hippocampal formation. Mol Psychiatry 10(7):631–636.

Tsai SJ, Hong CJ, Liu HC, Liu TY, Liou YJ. 2006. The brain-derived neurotrophic factor gene as a possible susceptibility candidate for Alzheimer's disease in a chinese population. Dement Geriatr Cogn Disord 21(3):139–143.

Ventriglia M, Bocchio Chiavetto L, Benussi L, Binetti G, Zanetti O, Riva MA, Gennarelli M. 2002. Association between the BDNF 196 A/G polymorphism and sporadic Alzheimer's disease. Mol Psychiatry 7(2):136–137.

Vepsalainen S, Castren E, Helisalmi S, Iivonen S, Mannermaa A, Lehtovirta M, Hanninen T, Soininen H, Hiltunen M. 2005. Genetic analysis of BDNF and TrkB gene polymorphisms in Alzheimer's disease. J Neurol 252(4):423–428.

Verhagen M, van der Meij A, van Deurzen PA, Janzing JG, Arias-Vasquez A, Buitelaar JK, Franke B. 2008. Meta-analysis of the BDNF Val66Met polymorphism in major depressive disorder: Effects of gender and ethnicity. Mol Psychiatry (in press).

Wenham PR, Price WH, Blandell G. 1991. Apolipoprotein E genotyping by one-stage PCR. Lancet 337(8750):1158–1159.

Zhang H, Ozbay F, Lappalainen J, Kranzler HR, van Dyck CH, Charney DS, Price LH, Southwick S, Yang BZ, Rasmussen A, et al. 2006. Brain derived neurotrophic factor (BDNF) gene variants and Alzheimer's disease, affective disorders, posttraumatic stress disorder, schizophrenia, and substance dependence. Am J Med Genet Part B 141B(4):387–393.

Zhang XM, Zhu SW, Duan RS, Mohammed AH, Winblad B, Zhu J. 2008. Gender differences in susceptibility to kainic acid-induced neurodegeneration in aged C57BL/6 mice. Neurotoxicology 29(3):406–412.

Neurochemistry International 54 (2009) 330–338

Contents lists available at ScienceDirect

Neurochemistry International

journal homepage: www.elsevier.com/locate/neuint

Proteomic and histochemical analysis of proteins involved in the dying-back-type of axonal degeneration in the gracile axonal dystrophy (*gad*) mouse

Akiko Goto [a,b], Yu-Lai Wang [a], Tomohiro Kabuta [a], Rieko Setsuie [a], Hitoshi Osaka [a], Akira Sawa [c], Shoichi Ishiura [b], Keiji Wada [a,*]

[a] *Department of Degenerative Neurological Diseases, National Institute of Neuroscience, National Center of Neurology and Psychiatry, 4-1-1 Ogawahigashi, Kodaira, Tokyo, 187-8502, Japan*
[b] *Department of Life Sciences, Graduate School of Arts and Sciences, University of Tokyo, 3-8-1 Komaba, Meguro-ku, Tokyo,153-8902, Japan*
[c] *Depts. of Psychiatry and Neuroscience, Johns Hopkins University School of Medicine, Baltimore, MD 21287, USA*

ARTICLE INFO

Article history:
Received 24 November 2008
Received in revised form 12 December 2008
Accepted 17 December 2008
Available online 25 December 2008

Keywords:
Axonal degeneration
Dying-back
gad mouse
UCH-L1
Ubiquitin
2D-DIGE
GAPDH
Oxidative stress

ABSTRACT

Local axonal degeneration is a common pathological feature of peripheral neuropathies and neurodegenerative disorders of the central nervous system, including Alzheimer's disease, Parkinson's disease, and stroke; however, the underlying molecular mechanism is not known. Here, we analyzed the gracile axonal dystrophy (*gad*) mouse, which displays the dying-back-type of axonal degeneration in sensory neurons, to find the molecules involved in the mechanism of axonal degeneration. The *gad* mouse is analogous to a null mutant of ubiquitin carboxyl-terminal hydrolase L1 (UCH-L1). UCH-L1 is a deubiquitinating enzyme expressed at high levels in neurons, as well as testis and ovary. In addition, we recently discovered a new function of UCH-L1—namely to bind to and stabilize mono-ubiquitin in neurons, and found that the level of mono-ubiquitin was decreased in neurons, especially in axons of the sciatic nerve, in *gad* mice. The low level of ubiquitin suggests that the target proteins of the ubiquitin proteasome system are not sufficiently ubiquitinated and thus degraded in the *gad* mouse; therefore, these proteins may be the key molecules involved in axonal degeneration. To identify molecules involved in axonal degeneration in *gad* mice, we compared protein expression in sciatic nerves between *gad* and wild-type mice at 2 and 12 weeks old, using two-dimensional difference gel electrophoresis. As a result, we found age-dependent accumulation of several proteins, including glyceraldehyde-3-phosphate dehydrogenase (GAPDH) and 14-3-3, in *gad* mice compared with wild-type mice. Histochemical analyses demonstrated that GAPDH and 14-3-3 were localized throughout axons in both *gad* and wild-type mice, but GAPDH accumulated in the axons of *gad* mice. Recently, it has been suggested that a wide range of neurodegenerative diseases are characterized by the accumulation of intracellular and extracellular protein aggregates, and it has been reported that oxidative stress causes the aggregation of GAPDH. Furthermore, histochemical analysis demonstrated that sulfonated GAPDH, a sensor of oxidative stress that elicits cellular dysfunction, was expressed in the axons of *gad* mice, and 4-hydroxy-2-nonenal, a major marker of oxidative stress, was also only detected in *gad* mice. Our findings suggest that GAPDH may participate in a process of the dying-back-type of axonal degeneration in *gad* mice and may provide valuable insight into the mechanisms of axonal degeneration.

1. Introduction

Axonal degeneration occurs in several chronic neurodegenerative diseases and in injuries caused by, for example, toxic, ischemic, or traumatic insults. Recent findings suggest that axonal degeneration precedes, and sometimes causes, neuronal death in these neurodegenerative disorders (Li et al., 2001; Ferri et al., 2003; Fischer et al., 2004; Stokin et al., 2005; Fischer and Glass, 2007), but the underlying molecular mechanism is not known.

The gracile axonal dystrophy (*gad*) mutant mouse is characterized by sensory ataxia at an early stage, followed by motor ataxia at a later stage (Yamazaki et al., 1988; Saigoh et al., 1999). Pathologically, axonal degeneration in the *gad* mouse begins with the distal ends of primary ascending axons in the dorsal root ganglia (DRG) (Mukoyama et al., 1989; Kikuchi et al., 1990; Oda et al., 1992; Miura et al., 1993), and spheroid formation in the dying-back-type of axonal degeneration is observed in the gracile and dorsal spinocerebellar tracts (Yamazaki et al., 1988; Kikuchi

* Corresponding author. Tel.: +81 42 346 1715 fax: +81 42 346 1745.
E-mail address: wada@ncnp.go.jp (K. Wada).

0197-0186/$ – see front matter © 2008 Elsevier Ltd. All rights reserved.
doi:10.1016/j.neuint.2008.12.012

et al., 1990; Miura et al., 1993). At a later stage, axonal degeneration and spheroid formation are observed at both the central and peripheral ends of DRG neurons and extend transsynaptically to the upper tracts as well as to motor neurons (Mukoyama et al., 1989; Kikuchi et al., 1990; Oda et al., 1992; Miura et al., 1993). Therefore, the *gad* mouse is an effective model for analyzing the molecular mechanism of the dying-back-type of axonal degeneration.

Previously, we found that the *gad* mutation is caused by an in-frame deletion of *Uchl1*, which encodes ubiquitin carboxyl-terminal hydrolase L1 (UCH-L1) (Saigoh et al., 1999). UCH-L1 is expressed at high levels in neurons, as well as testis and ovary, and constitutes ~5% of total soluble protein in the brain (Wilkinson et al., 1989). UCH-L1 is reported to be one of the deubiquitinating enzymes in the ubiquitin-proteasome system (UPS), where it hydrolyzes bonds between ubiquitin (Ub) and small adducts and creates free mono-Ub *in vitro* (Larsen et al., 1998). UCH-L1 also acts as a Ub ligase *in vitro* (Liu et al., 2002). In addition, we recently found a new function for UCH-L1—to bind to and stabilize mono-Ub in neurons (Osaka et al., 2003).

Using histochemical analysis, we previously demonstrated that UCH-L1 and mono-Ub are colocalized in axons of the sciatic nerve. In *gad* mice, the level of mono-Ub was decreased in neurons, especially in axons of the sciatic nerve (Osaka et al., 2003). The low level of ubiquitin suggests that the target proteins of the ubiquitin-proteasome system (UPS) are not sufficiently ubiquitinated and thus degraded in the *gad* mouse; therefore, these proteins may be key molecules involved in axonal degeneration. To identify the molecules involved in axonal degeneration in *gad* mice, we analyzed protein expression in sciatic nerves using two-dimensional difference gel electrophoresis (2D-DIGE).

Proteomic approaches compare protein expression comprehensively; 2D-DIGE is a modification of the traditional 2D technology, in which small amounts of multiple protein samples can be compared together, because each sample can be pre-labeled with different fluorescence dyes, mixed together, and run on the same isoelectric focusing (IEF) gel and SDS-PAGE (Knowles et al., 2003; Shaw and Riederer, 2003). We used 2D-DIGE because it is the most efficient method for analyzing the small amount of protein that can be extracted from a sciatic nerve. Here, we show that there are age-dependent accumulations of several proteins, including glyceraldehyde-3-phosphate dehydrogenase (GAPDH) and 14-3-3, in *gad* mice compared with wild-type (WT) mice, suggesting that these proteins are involved in axonal degeneration.

2. Experimental procedures

2.1. Animals

We used homozygous *gad* mice and their wild-type siblings (Harada et al., 2004; Wang et al., 2004). Mice were maintained and propagated at the National Institute of Neuroscience, National Center of Neurology and Psychiatry, Japan. Proteomic studies were carried out at 2 and 12 weeks old. Western blotting analyses were carried out at 12 weeks old. Histochemical analyses were carried out at 7 and 12 weeks old. Animals were anesthetized with Nembutal, and the sciatic nerve was perfused with saline. All mouse experiments were performed in accordance with our institution's regulations for animal care and with the approval of the Animal Investigation Committee of the National Institute of Neuroscience, National Center of Neurology and Psychiatry which conforms to the National Institute of Health guide for the care and use of laboratory animals.

2.2. Preparation of protein samples and labeling of protein samples with Cy dyes

Each sciatic nerve was suspended in 300 μl of sample buffer, containing 7 M urea, 2 M thiourea, 4% (w/v) CHAPS, and 40 mM Tris base (pH 8.0), by sonication for 60 s on ice, gently vortexed, and centrifuged for 20 min at 14,000 × *g* at 4 °C. Protein concentration was determined using a 2-D Quant Kit (GE Healthcare, Piscataway, NJ, USA). Protein samples were labeled as recommended by the manufacturer (GE Healthcare) using 400 pmol Cy dyes (GE Healthcare) per 50 μg of protein. Separate solutions containing 15 μg of protein from one *gad* or WT sample were labeled with Cy3 or Cy5 dye, respectively, and a common pool of proteins with *gad* and WT samples mixed equally were labeled with Cy2 dye by vortexing and incubating on ice in the dark for 30 min. The labeled samples were quenched by the addition of 1 μl 10 mM lysine (Sigma–Aldrich, St. Louis, MO, USA) and incubated on ice for 10 min.

2.3. Two-dimensional polyacrylamide gel electrophoresis (2D PAGE)

The quenched Cy3, Cy5, and Cy2 samples (15 μg of protein each) were mixed and denatured in 2D PAGE sample buffer containing 7 M urea, 2 M thiourea, 4% (w/v) CHAPS, 0.2% DTT, and 1.4% Ampholine. For the IEF, 45 μg of protein was applied to a rehydrated Immobiline Drystrip (pH 3–10, 7 cm; GE Healthcare) in a strip holder and incubated overnight in the dark. IEF was performed using a Multiphor II Electrophoresis system (GE Healthcare). The electrophoresis conditions were set as follows: step 1, 200 V for 1 min; step 2, 3500 V for 90 min; step 3, 3500 V for 125 min. After IEF, the strip was equilibrated with SDS buffer and applied to the 12.5% 2D SDS-PAGE for the analysis of 12-week-old mice and to the 4–20% SDS-PAGE for the analysis of 2-week-old mice using a precast Multigel II system (Daiichi Kagaku, Japan).

2.4. Image analysis and statistics

We scanned 2D gels using a Typhoon 9000 fluorescent imager (GE Healthcare). Excitation/emission wavelengths were chosen for each of the dyes. Gel images were preprocessed to remove extraneous areas using ImageQuant V5.0 (GE Healthcare). Gel analysis was performed using DeCyder DIA V5.0 (Difference In-gel Analysis; GE Healthcare). In-gel matching and statistical analysis were performed using DeCyder BVA V5.0 (Biological Variance Analysis; GE Healthcare). The Student's paired *t*-test ($P < 0.05$) was performed to identify the protein spots that were differentially expressed between *gad* and WT mice.

2.5. In-gel digestion and analysis by matrix-assisted laser desorption/ionization tandem time-of-flight (MALDI-TOF/TOF) mass spectrometry

To identify a particular protein in a spot detected by 2D-DIGE analysis, sciatic nerve extract containing 100 μg of protein was subjected to 12.5% 2D SDS-PAGE and stained with Coomassie brilliant blue (Invitrogen). The spots of interest were excised from the gel, destained, dehydrated with acetonitrile for 10 min, and completely dried under a vacuum pump for 10 min. Each spot was placed in 20 μl of 5 mM NH_4HCO_3 containing 1 pmol of sequencing-grade trypsin (Promega, Madison, WI, USA) overnight at 37 °C. Aliquots of the trypsinized samples were analyzed by nanoliquid chromatography and automatically spotted with alpha-cyano-4-hydroxy-cinnamic acid solution on a stainless-steel target and air dried. All mass spectra were obtained with MALDI-TOF/TOF (AXIMA-CFR; Shimadzu, Japan). MALDI peptide spectra were calibrated using several peaks of self-digested trypsin and matrix ion as internal standards.

2.6. Protein identification

Protein identification was performed using database searches on the web with Mascot Wizard (Matrix Science Ltd., London, United Kingdom). Criteria for protein identification were as follows: mascot score higher than 80 and mass tolerance of 100 ppm. Calculated pI and molecular mass data were obtained by Mascot.

2.7. 2D Western blotting for identification of GAPDH

One protein spot that was increased in *gad* mice but could not be detected by MALDI-TOF/TOF analysis was speculated to be GAPDH from its isoelectric point, molecular weight and location of the 2D gel compared with the mouse brain proteome database, and was therefore subjected to 2D Western blotting using an anti-GAPDH antibody (1:200, Chemicon, MAB374). One-hundred μg of sciatic nerve proteins were separated by 12.5% 2D SDS-PAGE and transferred onto a PVDF membrane (Immobilon-P; Millipore, Bedford, MA, USA). The membrane was washed with MilliQ water for 1 h at room temperature. Western blotting was performed as described in the following section.

2.8. Western blotting

Using 4–20% gradient SDS-PAGE, 2 μg of total protein was separated and transferred onto a PVDF membrane (Immobilon-P; Millipore). The membrane was washed with MilliQ water, then blocked with 5% skim milk in 0.05% Tween 20 in TBS (TTBS) for 1 h at room temperature, and incubated with primary antibodies in TTBS overnight at 4 °C. Primary antibodies used in this study were anti-UCH-L1 polyclonal antibody (1:5000, UltraClone, RA95101), anti-GAPDH monoclonal antibody (1:200, Chemicon, MAB374), anti-14-3-3 polyclonal antibody (1:100, IBL, 18649), anti-neurofilament L monoclonal antibody (NF-L, 1:500, Chemicon, MAB1615), anti-neuronal class III β tubulin antibody (βTUBIII, 1:1000, Covance, TUJ1), and anti-actin monoclonal antibody (1:4000, Sigma, AC-15). After washing, the membranes were incubated for 1 h at room temperature with either anti-mouse or anti-rabbit IgG horseradish peroxidase (HRP) conjugated secondary antibodies (1:10,000, GE Healthcare). Protein signals were detected with SuperSignal West Femto Maximum Sensitivity Substrate (Pierce) and were visualized with the LAS-3000 imaging system (Fujifilm, Tokyo, Japan).

2.9. Immunohistochemistry

Mice were anesthetized and perfused with ice-cold 4% paraformaldehyde in phosphate-buffered saline (PBS, pH 7.4). Sciatic nerves were collected and postfixed in 4% paraformaldehyde overnight at 4 °C. The samples were embedded in paraffin and sectioned at 5 μm for immunohistochemistry. Serial sections were deparaffinized in xylene and graded ethanol, and washed in distilled water. Sections were blocked by incubation in 10% normal goat serum for 30 min at room temperature and incubated overnight at 4 °C with diluted primary antibodies. The following antibodies were used at the final dilutions indicated: anti-GAPDH polyclonal antibody (1:1000), anti-sulfonated GAPDH polyclonal antibody (1:500; these two antibodies were kindly provided by Dr. Sawa), anti-14-3-3 polyclonal antibody (1:100, IBL, 18649), anti-myelin basic protein monoclonal antibody (MBP, 1:200, QED Bioscience, 24201), anti-neurofilament M monoclonal antibody (NF-M, 1:200, Chemicon, MAB1621), anti-UCH-L1 polyclonal antibody (1:2000, UltraClone, RA95101), anti-UCH-L1 monoclonal antibody (1:200; Medac, Wedel, Germany), βTUBIII (1:300, COVANCE, TUJ1), and anti-4-hydroxy-2-nonenal monoclonal antibody (HNE, 25 μg/ml, JalCA, Shizuoka, Japan).

After incubating with primary antibodies, sections were washed 5 times with 0.1% Tween 20 in PBS (PBST) for 5 min at room temperature and then incubated for 90 min at room temperature with diluted secondary antibodies. The following antibodies were used at the final dilutions indicated: anti-mouse-Alexa594 IgG and anti-rabbit-Alexa588 IgG (1:400, Invitrogen) for immunofluorescence staining, or EnVision+ anti-rabbit HRP (Dako, Japan) for DAB staining. For DAB staining, bound antibody complexes were visualized using DAB (Dako, Japan) as a peroxidase substrate. Primary and secondary antibodies were diluted in Dako Antibody Diluent (Dako, Japan). After incubation with secondary antibodies, sections were washed 5 times with PBST for 5 min at room temperature and mounted with Antifade Kit (Molecular Probes). For analysis of 14-3-3 and HNE, sections were pretreated in a microwave oven for 10 min in citrate buffer solution (pH 6.0), cooled down, and washed 3 times for 5 min in PBS at room temperature. For the other immunostaining analyses, this pretreatment was not needed. For DAB staining, sections were treated with 3% H_2O_2 in methanol for 5 min to quench endogenous peroxidase activity before treatment with the primary antibodies.

3. Results

3.1. Analyses of differentially expressed proteins between gad and WT mice by 2D-DIGE

To find proteins that are upregulated in *gad* mice compared with WT mice, we analyzed sciatic nerves from 3 *gad* and 3 WT mice at 2 weeks old as well as at 12 weeks old, using 2D-DIGE technology. The proteins from *gad* mice were pre-labeled with Cy5 (red), and the proteins from WT mice were pre-labeled with Cy3 (green), respectively. A common pool of proteins composed of an equal amount of protein from a single *gad* and WT mouse was pre-labeled with Cy2, and the same manipulation was performed in 3 independent experiments.

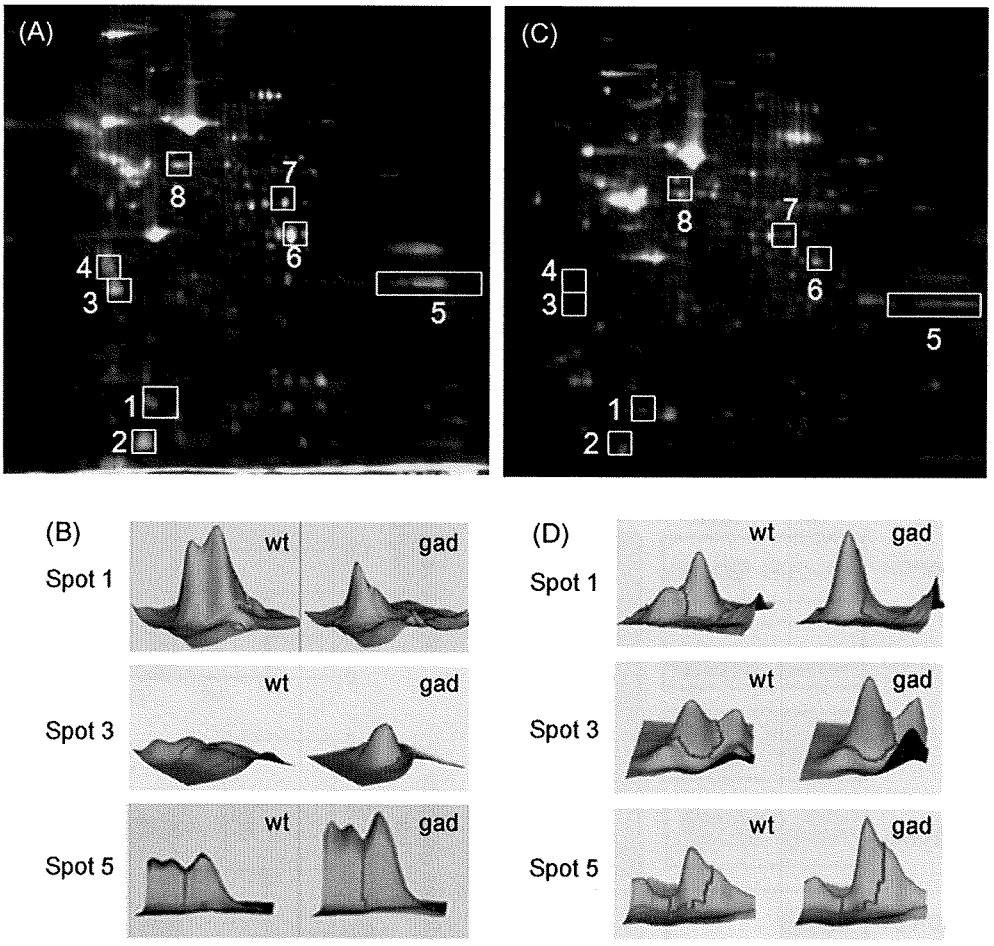

Fig. 1. Analyses of differentially expressed proteins between *gad* and wild-type mice by two-dimensional difference gel electrophoresis (2D-DIGE).
(A) A representative pseudocolor picture of superimposed DIGE images of mice at 12 weeks old. Fourteen protein spots are increased in *gad* mice compared with wild-type (WT) mice (red) by at least 1.6-fold (Student's paired *t*-test value; $P < 0.05$ in 3 parallel gels), and one spot is not detected at all in *gad* mice (green). Seven protein spots (spot No. 2–8) are increased in *gad* mice in an age-dependent manner, and one spot (spot No. 1) was not detected at all in *gad* mice at either 2 or 12 weeks old. The spot numbers of the latter differentiated 8 spots are shown in this map.
(B) A representative pseudocolor picture of superimposed DIGE images of mice at 2 weeks old. Eighteen protein spots are increased in *gad* mice compared with WT mice (red) by at least 1.6-fold (Student's paired *t*-test value; $P < 0.05$ in 3 parallel gels), and one spot is not detected at all in *gad* mice (green). The spot numbers in this figure are the same as in A.
(C) The 3D images of typical protein spots that were differentially expressed between *gad* and WT mice at 2 weeks old (spot numbers 1, 3, and 5 in A).
(D) The 3D images of typical protein spots that were differentially expressed between *gad* and WT mice at 2 weeks old (spot numbers 1, 3, and 5 in C) (For interpretation of the references to color in this figure legend, the reader is referred to the web version of the article.)

Table 1
List of proteins differentially expressed between *gad* and WT mice.

Spot no.	Protein name	Score	Molecular mass (kDa)/pI	Av. ratio (*gad*/wt) 12 weeks	*P* value	Av. ratio (*gad*/wt) 2 weeks	*P* value
1	Ubiquitin thiolesterase PGP9.5 (UCH-L1)	96	25.10/5.12	−14.38	0.005	−3.89	0.003
3	14-3-3 protein	94	28.10/4.63	5.4	0.030	7.32	0.001
4	Annexin A5	143	35.79/4.83	6.68	0.020	5.19	0.030
8	Neurofilament triplet L protein (NF-L)	212	61.40/4.62	2.18	0.010	3.53	0.026
5	Glyceraldehyde 3-phosphate dehydrogenase (GAPDH)		38.07/8.34	3.89	0.043	1.61	

*GAPDH was detected by 2D Western blotting and not by MALDI-TOF/TOF.

Fig. 1A shows a representative pseudocolor picture of superimposed DIGE images of the 12-week-old mouse samples. Fourteen protein spots were increased by at least 1.6-fold in *gad* mice compared with WT mice (red; Student's paired *t*-test value; $P < 0.05$ in 3 parallel gels), and one spot was not detected at all in *gad* mice (green).

Fig. 1B shows a representative pseudocolor picture of superimposed DIGE images of the 2-week-old mouse samples. Eighteen protein spots were increased by at least 1.6-fold in *gad* mice compared with WT mice (red; Student's paired *t*-test value; $P < 0.05$ in 3 parallel gels), and one spot was not detected at all in *gad* mice (green).

Based on comparison of the 2D-DIGE analysis of mice between 2 and 12 weeks old, 7 protein spots showed an age-dependent increase in *gad* mice (spots No. 2–8). One spot (spot No. 1) was not detected at all in *gad* mice at either 2 or 12 weeks old (Fig. 1A and B).

Fig. 1C shows the 3D images of typical spots (spots No. 1, 3, and 5) in Fig. 1A, and Fig. 1D shows the 3D images of typical spots (spots No. 1, 3, and 5) in Fig. 1B.

3.2. Identification of differentially expressed proteins between gad and WT mice by MALDI-TOF/TOF and 2D Western blotting

The proteins of spots that were age dependently increased or absent in *gad* mice were analyzed by MALDI-TOF/TOF and identified (spots No. 1, 3, 4, and 8). The proteins were identified as UCH-L1 (spot No. 1), 14-3-3 (spot No. 3), annexin V (spot No. 4), and Neurofilament L (NF-L) (spot No. 8). Additionally, we speculated that spot No. 5 may represent GAPDH based on the information from the mouse brain proteome database (http://www.charite.de/humangenetik/klose_public1/index.html), and confirmed this by 2D Western blotting with GAPDH antibodies. The results of the protein identification are listed in Table 1, including spot number, protein name, mascot score, theoretical relative molecular mass, isoelectric point, average ratio of *gad*/wt protein level, and *P*-value using DeCyder, at both 2 and 12 weeks old.

3.3. Analyses of the expression levels of proteins in gad and WT mice by Western blotting

In 2D-DIGE system, each sample was pre-labeled with different fluorescence dyes, Cy3, Cy5 or Cy2. This labeling-process allows comparison of multiple samples in same 2D-gel, but it is reported that efficiency of each dyes to label proteins was not exactly the same. We assume that 2D-DIGE is reliable method to detect molecules involved in axonal degeneration but Western blot analysis using specific antibodies is more accurate, and in fact, it is usual that identified proteins by TOF-MASS are reconfirmed by Western blotting. Therefore, the expression levels of the proteins in

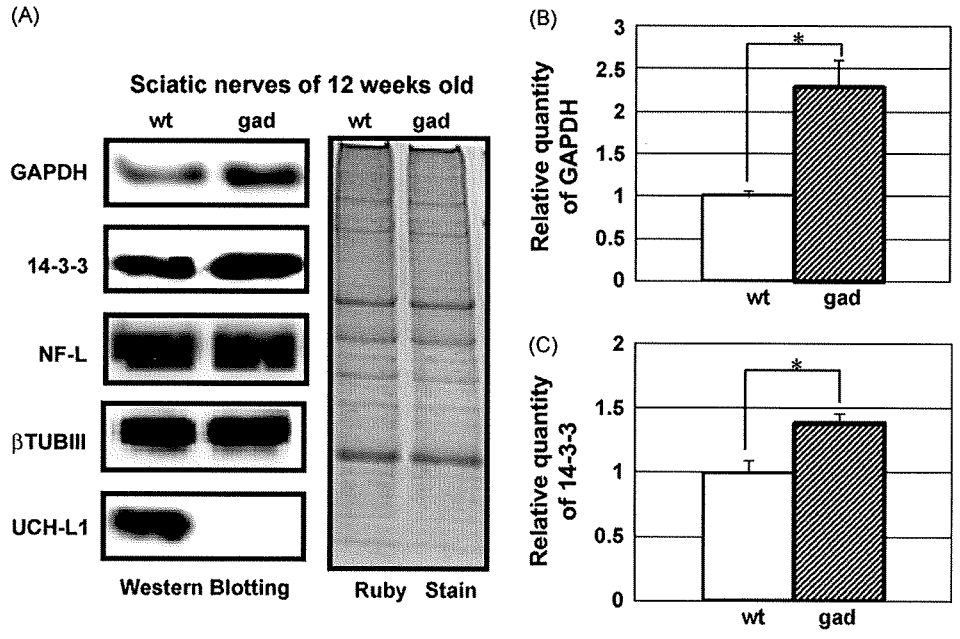

Fig. 2. Western blotting analyses of the expression levels of proteins expressed differentially between *gad* and WT mice.
(A) Results of Western blotting analysis with antibodies against ubiquitin carboxyl-terminal hydrolase L1 (UCH-L1), neurofilament L (NF-L), 14-3-3, glyceraldehyde-3-phosphate dehydrogenase (GAPDH), and classIII β tubulin (βTUBIII). GAPDH and 14-3-3 protein levels were increased in *gad* mice compared with WT mice.
(B) Quantification of the band intensities of GAPDH. Values are means ± SEM of 3 independent experiments (*$P < 0.05$); GAPDH is increased by about 2.3-fold in *gad* mice at 12 weeks old compared with WT mice.
(C) Quantification of the band intensities of 14-3-3. Values are means ± SEM of 3 independent experiments (*$P < 0.05$); 14-3-3 is increased by 1.3-fold in *gad* mice at 12 weeks old compared with WT mice.

gad and WT mice listed in Table 1 were further analyzed by Western blotting to reconfirm the results of 2D-DIGE (Fig. 2A). We chose these proteins because they were all reported to be expressed in neurons. In 12-week-old *gad* mice, GAPDH was increased by an average ratio of 2.3-fold (Fig. 2B), and 14-3-3 was increased by an average ratio of 1.3-fold (Fig. 2C) compared with WT mice. The levels of NF-L and βTUBIII, which was used as an internal control, showed no significant difference between *gad* and WT mice at 12 weeks old (Fig. 2A). Annexin V was not analyzed because its antibodies did not work in this experimental system containing urea and thiourea. The same results were obtained in 3 independent experiments.

3.4. Histochemical localization of GAPDH in the sciatic nerves of gad and WT mice

Sciatic nerves are composed internally of neuronal axons and externally of myelin derived from glial Schwann cells, and protein samples in the proteomic analysis were a mixture of axons and myelin. We examined the histological localization of GAPDH, which was dominantly increased in *gad* mice, by double immunofluorescence staining using an antibody against GAPDH and the neuronal markers neurofilament M (NF-M) or UCH-L1, or the Schwann cells marker myelin basic protein (MBP). In *gad* mice, GAPDH was colocalized with MBP (Fig. 3A, right panel) but was more dominantly colocalized with NF-M, a neuronal marker (Fig. 3A, left panel). These results suggest that GAPDH is mainly localized in axons in *gad* mice. In WT mice, GAPDH was colocalized with the neuronal marker UCH-L1 (Fig. 3B, left panel). Because UCH-L1 is the product of the gene defective in the *gad* mouse, UCH-L1 is not detected in *gad* mice (Fig. 3B, right panel). The same results were obtained in 3 independent experiments.

3.5. DAB staining analyses of GAPDH and 14-3-3 in the sciatic nerves of gad and WT mice

We examined in detail the localization of GAPDH in cross or vertical sections of sciatic nerve axons by DAB staining (Figs. 4A–F). In the cross-sections, GAPDH was localized in axons in both *gad* and WT mice and was remarkably accumulated in *gad* mice compared with WT mice (Fig. 4A and B). In vertical sections, GAPDH was also localized in axons in both *gad* and WT mice (Fig. 4C–F). Notably, aggregates of GAPDH were observed in *gad* mice but not in WT mice (Fig. 4E and F, arrow). Next, we examined the expression of 14-3-3, which was found to be increased in *gad* mice upon 2D-DIGE and Western blotting analyses. In both *gad* and WT mice, 14-3-3 was expressed in axons, and there was no significant difference between *gad* and WT mice (Fig. 4G–J). The same results were obtained in 3 independent experiments.

3.6. Histochemical analyses of sulfonated GAPDH in the sciatic nerves of gad and WT mice

It was reported that oxidative stress induces the oligomerization and aggregation of GAPDH (Cumming and Schubert, 2005; Nakajima et al., 2007), and in this study we found that GAPDH is accumulated in axons of *gad* mice that exhibit a dying-back-type of axonal degeneration. Thus, we postulated that oxidative stress would be increased in *gad* mice, and therefore examined the expression of sulfonated GAPDH (Hara et al., 2005), in the sciatic

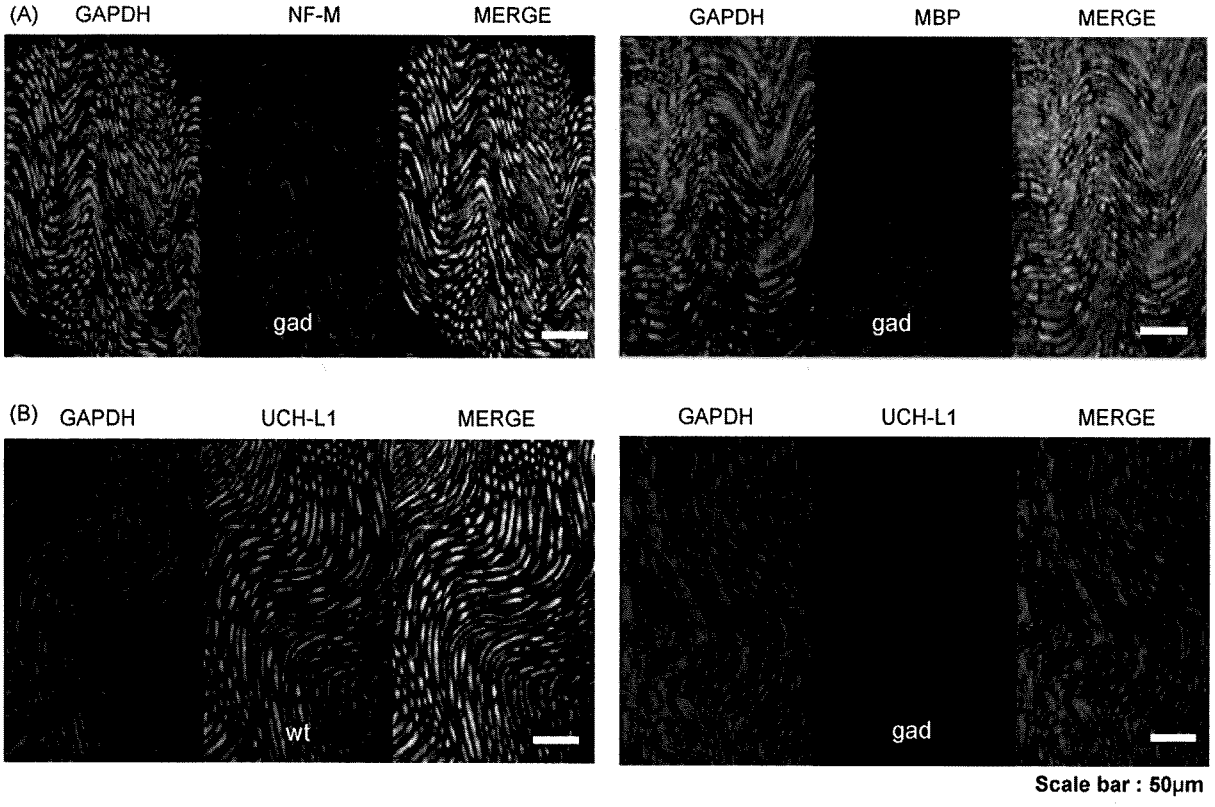

Fig. 3. Histochemical localization of GAPDH in the sciatic nerves of *gad* and WT mice.
(A) Double immunofluorescent staining of the sciatic nerve of *gad* mice using antibodies against GAPDH, neurofilament M (NF-M), or myelin basic protein (MBP). GAPDH was colocalized with NF-M (left panel) and partly with MBP (right panel) in *gad* mice. GAPDH is mainly localized in axons.
(B) Double immunofluorescent staining of the sciatic nerve of *gad* and WT mice using antibodies against GAPDH and UCH-L1. In WT mice, GAPDH is colocalized with UCH-L1 (left panel). In *gad* mice, UCH-L1 is not detected (right panel), and GAPDH is strongly detected compared with WT mice.

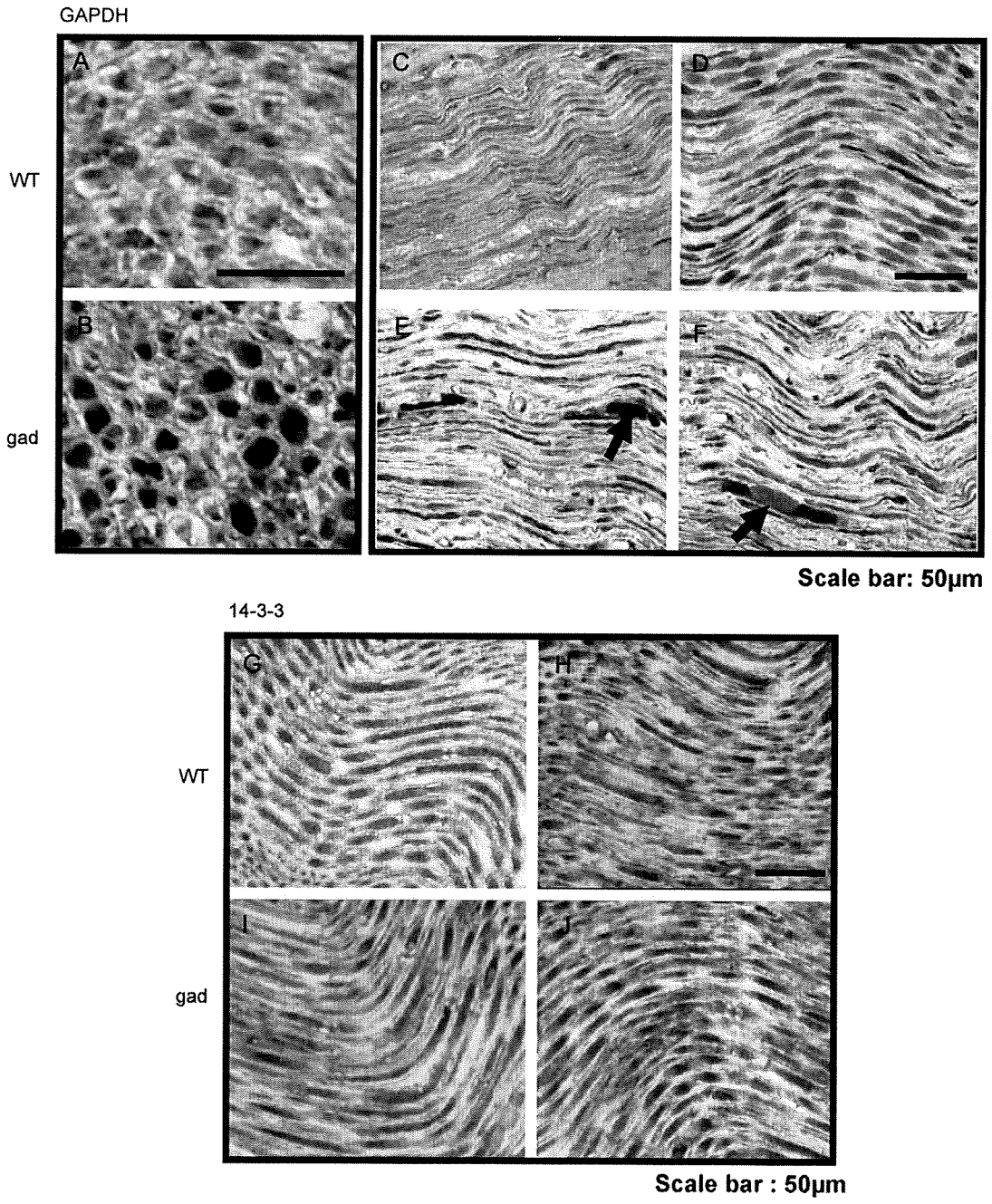

Fig. 4. DAB staining of GAPDH and 14-3-3 in the sciatic nerves of *gad* and WT mice.
(A–F) Sections of sciatic nerves of WT (A, C, and D) or *gad* (B, E, and F) mice stained with DAB using GAPDH antibodies.
(A) Cross-section of a sciatic nerve of a WT mouse. GAPDH is mainly localized in axons.
(B) Cross-section of a sciatic nerve of a *gad* mouse. GAPDH is mainly localized in axons and is highly expressed compared with the WT mouse.
(C and D) Vertical sections of sciatic nerves of WT mice. GAPDH is localized in axons.
(E and F) Vertical sections of sciatic nerves of *gad* mice. GAPDH is localized in axons and is accumulated. GAPDH aggregates are indicated by arrows.
(G–J) Sections of sciatic nerves of WT (G, H) and *gad* (I, J) mice stained with DAB using 14-3-3 antibodies.
(G and H) Vertical sections of sciatic nerves of WT mice; 14-3-3 is localized in axons of WT mice.
(I and J) Vertical sections of sciatic nerves of *gad* mice; 14-3-3 is localized in axons of *gad* mice, and there was no significant difference between *gad* and WT mice (G, H).

nerves of *gad* and WT mice. We found that although sulfonated GAPDH was not detected in WT mice, it was clearly detected in *gad* mice (Fig. 5A and B). In *gad* mice, sulfonated GAPDH was colocalized with the neuronal markers βTUBIII (Fig. 5B) and NF-M (data not shown) in axons. In *gad* mice, accumulated sulfonated GAPDH was also detected in the outer portion of the axons, around the DAPI staining for nuclei (Fig. 5C). Axons do not contain nuclei, so these DAPI signals may come from Schwann cells. The same results were obtained in 3 independent experiments.

3.7. Histological analyses of HNE, a marker of oxidative stress, in the sciatic nerves of gad and WT mice

The results shown in Fig. 5 suggest that the level of oxidative stress is increased in *gad* mice. Accordingly, we examined the existence of HNE, a major marker of oxidative stress, in addition to sulfonated GAPDH. HNE was detected in *gad* mice, but not in WT mice (Fig. 6). The same results were obtained in 3 independent experiments.

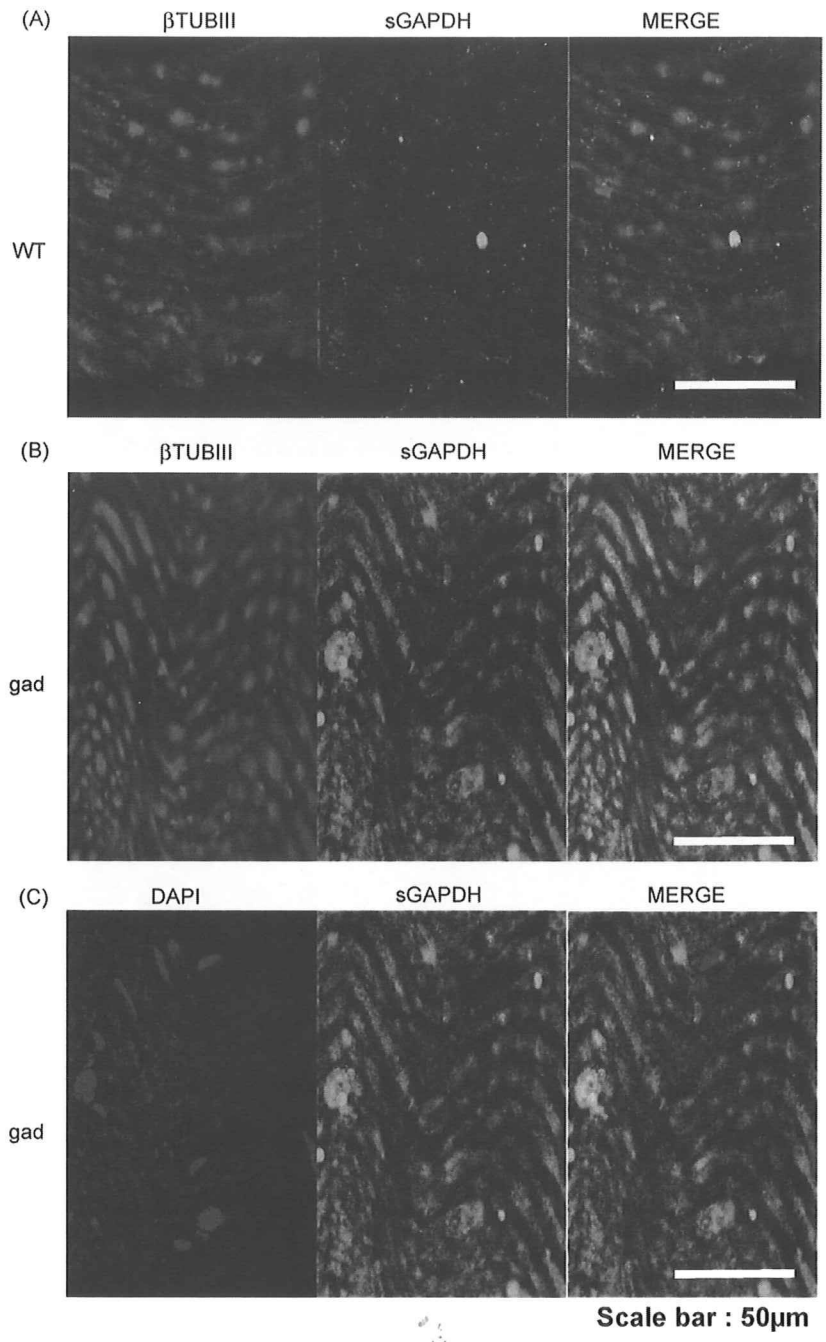

Fig. 5. Expression of sulfonated GAPDH in the sciatic nerves of *gad* and WT mice.
(A) Double immunofluorescent staining of a sciatic nerve of a WT mouse using antibodies against sulfonated GAPDH and βTUBIII. Sulfonated GAPDH was not detected in WT mice (middle panel).
(B) Double immunofluorescent staining of a sciatic nerve of a *gad* mouse using antibodies against sulfonated GAPDH and βTUBIII. In *gad* mice, sulfonated GAPDH was detected in axons of sciatic nerves (middle panel). Sulfonated GAPDH was colocalized with the neuronal marker βTUBIII in *gad* mice (right panel), as well as NF-M (data not shown). A representative result from 3 independent experiments is shown.
(C) Double immunofluorescent staining of a sciatic nerve of the *gad* mouse using an antibody against sulfonated GAPDH and DAPI. Sulfonated GAPDH was detected uniformaly within the axons of *gad* mice, and accumulation of sulfonated GAPDH was detected around the DAPI signals (right panel).

4. Discussion

In this study, we found that 14-3-3, annexin V, NF-L, and GAPDH were increased in an age-dependent manner in *gad* mice that display the dying-back-type of axonal degeneration, using 2D-DIGE analyses (Fig. 1). Based on Western blotting analyses, 14-3-3 and GAPDH were increased in *gad* mice compared with WT mice (Fig. 2). Histochemical analysis revealed that GAPDH was localized throughout axons and was accumulated in axons in *gad* mice compared with WT mice (Figs. 3 and 4). Also 14-3-3 was localized throughout axons, but there was no significant difference between *gad* and WT mice upon histochemical analyses, although it was increased in *gad* mice upon Western blotting analyses (Fig. 4). Since Western blotting showed only a slight increase in 14-3-3 (Fig. 2), we assume that this small difference could not be detected by histochemical analyses.

GAPDH is a classic glycolytic enzyme (Sirover, 1999; Chuang et al., 2005), and recent studies show that it is multifunctional

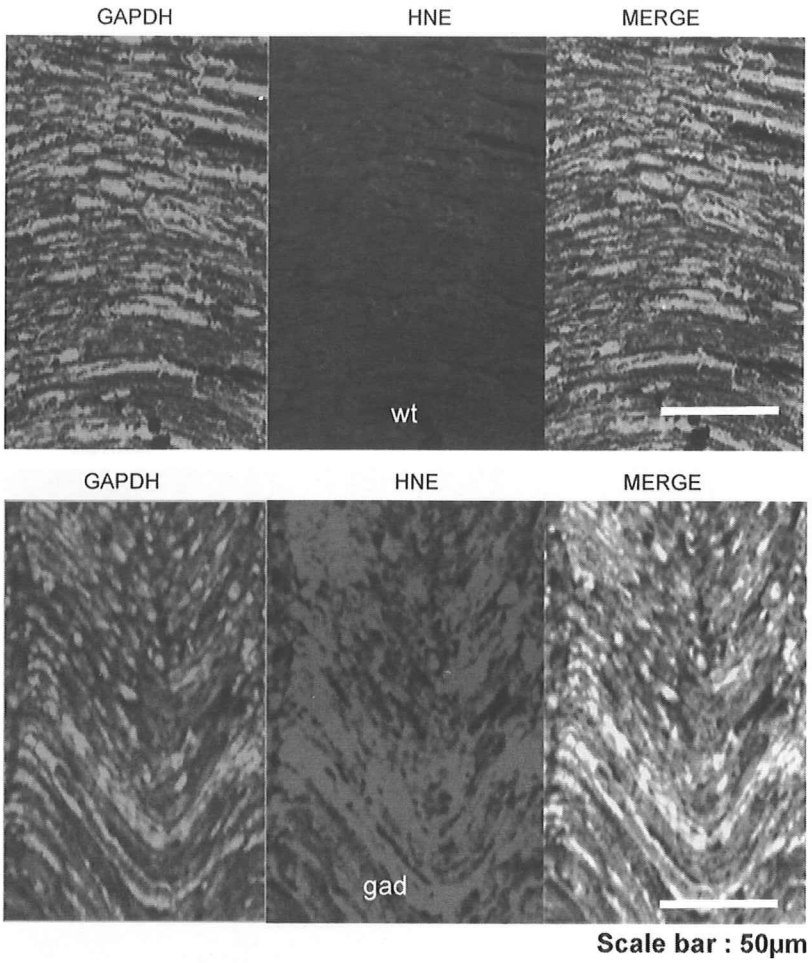

Fig. 6. Expression of HNE, a marker of oxidative stress, in the sciatic nerves of *gad* and WT mice.
Double immunofluorescent staining of sciatic nerves of *gad* and WT mice using antibodies against GAPDH and HNE. In WT mice, HNE was not detected (upper panel). On the other hand, HNE was strongly detected and mainly colocalized with GAPDH in *gad* mice (lower panel).

(Hara et al., 2006a). GAPDH has been reported to play roles in membrane fusion, microtubule bundling, nuclear RNA transport (Sirover, 1999), and transcription (Zheng et al., 2003). Particularly, its role as a mediator for cellular dysfunction/death has been highlighted (Sawa et al., 1997; Ishitani et al., 1998; Hara et al., 2005, 2006b). Sulfonation of GAPDH is reported to be induced by oxidative stress, and sulfonated GAPDH leads to cellular dysfunction (Hara et al., 2005, 2006a; Sen et al., 2008). Additionally, oxidative stress induces the oligomerization and aggregation of GAPDH through aberrant disulfide bonding of active-site cysteines, which leads to the formation of insoluble aggregates *in vitro* (Cumming and Schubert, 2005; Nakajima et al., 2007). Thus, GAPDH appears to participate in the mechanism leading to cellular dysfunction/death induced by oxidative stress. However, its function in axons or its association with axonal degeneration has not yet been demonstrated.

In this study, we found that GAPDH and sulfonated GAPDH were accumulated in *gad* mice compared with WT mice, suggesting that oxidative stress is increased in *gad* mice. In fact, we found that the oxidative stress marker HNE is increased in *gad* mice. It has also been reported that, the levels of carbonyl modification of proteins that is caused by oxidative stress are increased in the brains of *gad* mice compared with WT mice (Castegna et al., 2004). Therefore, we assume that accumulation of GAPDH and sulfonated GAPDH in the axons of *gad* mice were induced by oxidative stress.

Various molecules are involved in reduction-oxidative reactions, and recently the necessity of the UPS in reduction-oxidative reactions has been highlighted (Okada et al., 1999; Kang et al., 2008). It has been reported that a number of oxidative stress sensors are regulated by the UPS (Iwai, 2003; Kobayashi et al., 2004; Hara et al., 2006a). In *gad* mice, free-Ub pools are decreased in neurons, and proteolysis in the UPS is thought to be abnormal (Osaka et al., 2003). Oxidative stress is therefore expected to be increased in *gad* mice, which is consistent with our findings.

There is another possible mechanism for the accumulation of GAPDH in the axons of *gad* mice. GAPDH is reported to be degraded mainly by chaperone-mediated autophagy (Aniento et al., 1993; Cuervo et al., 1997). Our recent study showed that UCH-L1 physically interacts with lysosome-associated membrane protein type 2A, which is a component of CMA (Kabuta et al., 2008); thus CMA is possibly altered in the neuronal system of *gad* mice, potentially leading to the accumulation of GAPDH in the axons of *gad* mice.

This study demonstrates the alteration of GAPDH in axons of the *gad* mouse, a mutant with a loss of function of UCH-L1. Our findings suggest that GAPDH may participate in the process leading to the dying-back-type of axonal degeneration in *gad* mice and may provide valuable insight into the mechanisms of axonal degeneration.

Acknowledgements

We thank the following people for their contributions to this work: Dr. Hidemitsu Nakajima (Osaka Prefecture University), Dr. Satoshi Nagamine (National Center of Neurology and Psychiatry) and Dr. Makoto R. Hara (Johns Hopkins University School of Medicine) for helpful discussions; Ms. Hisae Kikuchi (National Center of Neurology and Psychiatry) for technical assistance with tissue sections; Ms. Masako Shikama (National Center of Neurology and Psychiatry) for the care and breeding of animals; Dr. Hayato Onishi (University of Tokyo) for assistance with the TOF MASS analysis; and Dr. H. Akiko Popiel (National Center of Neurology and Psychiatry) for support with English; Mitsubishi Tanabe Pharma Corporation for giving a chance to A.G. of admission to doctoral course. This work was supported in part by Grants-in-Aid for Scientific Research from the Ministry of Health, Labour and Welfare of Japan, Grants-in-Aid for Scientific Research from the Ministry of Education, Culture, Sports, Science and Technology of Japan, the Program for Promotion of Fundamental Studies in Health Sciences of the National Institute of Biomedical Innovation, and a grant from Japan Science and Technology Agency.

References

Aniento, F., Roche, E., Cuervo, A.M., Knecht, E., 1993. Uptake and degradation of glyceraldehyde-3-phosphate dehydrogenase by rat liver lysosomes. J. Biol. Chem. 268, 10463–10470.

Castegna, A., Thongboonkerd, V., Klein, J., Lynn, B.C., Wang, Y.L., Osaka, H., Wada, K., Butterfield, D.A., 2004. Proteomic analysis of brain proteins in the gracile axonal dystrophy (gad) mouse, a syndrome that emanates from dysfunctional ubiquitin carboxyl-terminal hydrolase L-1, reveals oxidation of key proteins. J. Neurochem. 88, 1540–1546.

Chuang, D.M., Hough, C., Senatorov, V.V., 2005. Glyceraldehyde-3-phosphate dehydrogenase, apoptosis, and neurodegenerative diseases. Annu. Rev. Pharmacol. Toxicol. 45, 269–290.

Cuervo, A.M., Dice, J.F., Knecht, E., 1997. A population of rat liver lysosomes responsible for the selective uptake and degradation of cytosolic proteins. J. Biol. Chem. 272, 5606–5615.

Cumming, R.C., Schubert, D., 2005. Amyloid-beta induces disulfide bonding and aggregation of GAPDH in Alzheimer's disease. FASEB J. 19, 2060–2062.

Ferri, A., Sanes, J.R., Coleman, M.P., Cunningham, J.M., Kato, A.C., 2003. Inhibiting axon degeneration and synapse loss attenuates apoptosis and disease progression in a mouse model of motoneuron disease. Curr. Biol. 13, 669–673.

Fischer, L.R., Culver, D.G., Tennant, P., Davis, A.A., Wang, M., Castellano-Sanchez, A., Khan, J., Polak, M.A., Glass, J.D., 2004. Amyotrophic lateral sclerosis is a distal axonopathy: evidence in mice and man. Exp. Neurol. 185, 232–240.

Fischer, L.R., Glass, J.D., 2007. Axonal degeneration in motor neuron disease. Neurodegener. Dis. 4, 431–442.

Hara, M.R., Agrawal, N., Kim, S.F., Cascio, M.B., Fujimuro, M., Ozeki, Y., Takahashi, M., Cheah, J.H., Tankou, S.K., Hester, L.D., Ferris, C.D., Hayward, S.D., Snyder, S.H., Sawa, A., 2005. S-nitrosylated GAPDH initiates apoptotic cell death by nuclear translocation following Siah1 binding. Nat. Cell. Biol. 7, 665–674.

Hara, M.R., Cascio, M.B., Sawa, A., 2006a. GAPDH as a sensor of NO stress. Biochim. Biophys. Acta 1762, 502–509.

Hara, M.R., Thomas, B., Cascio, M.B., Bae, B.I., Hester, L.D., Dawson, V.L., Dawson, T.M., Sawa, A., Snyder, S.H., 2006b. Neuroprotection by pharmacologic blockade of the GAPDH death cascade. Proc. Natl. Acad. Sci. U.S.A. 103, 3887–3889.

Harada, T., Harada, C., Wang, Y.L., Osaka, H., Amanai, K., Tanaka, K., Takizawa, S., Setsuie, R., Sakurai, M., Sato, Y., Noda, M., Wada, K., 2004. Role of ubiquitin carboxy terminal hydrolase-L1 in neural cell apoptosis induced by ischemic retinal injury in vivo. Am. J. Pathol. 164, 59–64.

Ishitani, R., Tanaka, M., Sunaga, K., Katsube, N., Chuang, D.M., 1998. Nuclear localization of overexpressed glyceraldehyde-3-phosphate dehydrogenase in cultured cerebellar neurons undergoing apoptosis. Mol. Pharmacol. 53, 701–707.

Iwai, K., 2003. An ubiquitin ligase recognizing a protein oxidized by iron: implications for the turnover of oxidatively damaged proteins. J. Biochem. 134, 175–182.

Kabuta, T., Furuta, A., Aoki, S., Furuta, K., Wada, K., 2008. Aberrant interaction between Parkinson disease-associated mutant UCH-L1 and the lysosomal receptor for chaperone-mediated autophagy. J. Biol. Chem. 283, 23731–23738.

Kang, S.I., Choi, H.W., Kim, I.Y., 2008. Redox-mediated modification of PLZF by SUMO-1 and ubiquitin. Biochem. Biophys. Res. Commun. 369, 1209–1214.

Kikuchi, T., Mukoyama, M., Yamazaki, K., Moriya, H., 1990. Axonal degeneration of ascending sensory neurons in gracile axonal dystrophy mutant mouse. Acta Neuropathol. 80, 145–151.

Knowles, M.R., Cervino, S., Skynner, H.A., Hunt, S.P., de Felipe, C., Salim, K., Meneses-Lorente, G., McAllister, G., Guest, P.C., 2003. Multiplex proteomic analysis by two-dimensional differential in-gel electrophoresis. Proteomics 3, 1162–1171.

Kobayashi, A., Kang, M.I., Okawa, H., Ohtsuji, M., Zenke, Y., Chiba, T., Igarashi, K., Yamamoto, M., 2004. Oxidative stress sensor Keap1 functions as an adaptor for Cul3-based E3 ligase to regulate proteasomal degradation of Nrf2. Mol. Cell. Biol. 24, 7130–7139.

Larsen, C.N., Krantz, B.A., Wilkinson, K.D., 1998. Substrate specificity of deubiquitinating enzymes: ubiquitin C-terminal hydrolases. Biochemistry 37, 3358–3368.

Li, H., Li, S.H., Yu, Z.X., Shelbourne, P., Li, X.J., 2001. Huntingtin aggregate-associated axonal degeneration is an early pathological event in Huntington's disease mice. J. Neurosci. 21, 8473–8481.

Liu, Y., Fallon, L., Lashuel, H.A., Liu, Z., Lansbury Jr., P.T., 2002. The UCH-L1 gene encodes two opposing enzymatic activities that affect alpha-synuclein degradation and Parkinson's disease susceptibility. Cell 111, 209–218.

Miura, H., Oda, K., Endo, C., Yamazaki, K., Shibasaki, H., Kikuchi, T., 1993. Progressive degeneration of motor nerve terminals in GAD mutant mouse with hereditary sensory axonopathy. Neuropathol. Appl. Neurobiol. 19, 41–51.

Mukoyama, M., Yamazaki, K., Kikuchi, T., Tomita, T., 1989. Neuropathology of gracile axonal dystrophy (GAD) mouse. An animal model of central distal axonopathy in primary sensory neurons. Acta Neuropathol. 79, 294–299.

Nakajima, H., Amano, W., Fujita, A., Fukuhara, A., Azuma, Y.T., Hata, F., Inui, T., Takeuchi, T., 2007. The active site cysteine of the proapoptotic protein glyceraldehyde-3-phosphate dehydrogenase is essential in oxidative stress-induced aggregation and cell death. J. Biol. Chem. 282, 26562–26574.

Oda, K., Yamazaki, K., Miura, H., Shibasaki, H., Kikuchi, T., 1992. Dying back type axonal degeneration of sensory nerve terminals in muscle spindles of the gracile axonal dystrophy (GAD) mutant mouse. Neuropathol. Appl. Neurobiol. 18, 265–281.

Okada, K., Wangpoengtrakul, C., Osawa, T., Toyokuni, S., Tanaka, K., Uchida, K., 1999. 4-Hydroxy-2-nonenal-mediated impairment of intracellular proteolysis during oxidative stress. Identification of proteasomes as target molecules. J. Biol. Chem. 274, 23787–23793.

Osaka, H., Wang, Y.L., Takada, K., Takizawa, S., Setsuie, R., Li, H., Sato, Y., Nishikawa, K., Sun, Y.J., Sakurai, M., Harada, T., Hara, Y., Kimura, I., Chiba, S., Namikawa, K., Kiyama, H., Noda, M., Aoki, S., Wada, K., 2003. Ubiquitin carboxy-terminal hydrolase L1 binds to and stabilizes monoubiquitin in neuron. Hum. Mol. Genet. 12, 1945–1958.

Saigoh, K., Wang, Y.L., Suh, J.G., Yamanishi, T., Sakai, Y., Kiyosawa, H., Harada, T., Ichihara, N., Wakana, S., Kikuchi, T., Wada, K., 1999. Intragenic deletion in the gene encoding ubiquitin carboxy-terminal hydrolase in gad mice. Nat. Genet. 23, 47–51.

Sawa, A., Khan, A.A., Hester, L.D., Snyder, S.H., 1997. Glyceraldehyde-3-phosphate dehydrogenase: nuclear translocation participates in neuronal and nonneuronal cell death. Proc. Natl. Acad. Sci. U.S.A. 94, 11669–11674.

Sen, N., Hara, M.R., Kornberg, M.D., Cascio, M.B., Bae, B.I., Shahani, N., Thomas, B., Dawson, T.M., Dawson, V.L., Snyder, S.H., Sawa, A., 2008. Nitric oxide-induced nuclear GAPDH activates p300/CBP and mediates apoptosis. Nat. Cell. Biol. 10, 866–873.

Shaw, M.M., Riederer, B.M., 2003. Sample preparation for two-dimensional gel electrophoresis. Proteomics 3, 1408–1417.

Sirover, M.A., 1999. New insights into an old protein: the functional diversity of mammalian glyceraldehyde-3-phosphate dehydrogenase. Biochim. Biophys. Acta 1432, 159–184.

Stokin, G.B., Lillo, C., Falzone, T.L., Brusch, R.G., Rockenstein, E., Mount, S.L., Raman, R., Davies, P., Masliah, E., Williams, D.S., Goldstein, L.S., 2005. Axonopathy and transport deficits early in the pathogenesis of Alzheimer's disease. Science 307, 1282–1288.

Wang, Y.L., Takeda, A., Osaka, H., Hara, Y., Furuta, A., Setsuie, R., Sun, Y.J., Kwon, J., Sato, Y., Sakurai, M., Noda, M., Yoshikawa, Y., Wada, K., 2004. Accumulation of beta- and gamma-synucleins in the ubiquitin carboxyl-terminal hydrolase L1-deficient gad mouse. Brain Res. 1019, 1–9.

Wilkinson, K.D., Lee, K.M., Deshpande, S., Duerksen-Hughes, P., Boss, J.M., Pohl, J., 1989. The neuron-specific protein PGP 9.5 is a ubiquitin carboxyl-terminal hydrolase. Science 246, 670–673.

Yamazaki, K., Wakasugi, N., Tomita, T., Kikuchi, T., Mukoyama, M., Ando, K., 1988. Gracile axonal dystrophy (GAD), a new neurological mutant in the mouse. Proc. Soc. Exp. Biol. Med. 187, 209–215.

Zheng, L., Roeder, R.G., Luo, Y., 2003. S phase activation of the histone H2B promoter by OCA-S, a coactivator complex that contains GAPDH as a key component. Cell 114, 255–266.

J Neuropathol Exp Neurol

Vol. 68, No. 9
September 2009
pp. 994–1005

ORIGINAL ARTICLE

Abnormal Localization of Leucine-Rich Repeat Kinase 2 to the Endosomal-Lysosomal Compartment in Lewy Body Disease

Shinji Higashi, MD, PhD, Darren J. Moore, PhD, Ryoko Yamamoto, MD, PhD, Michiko Minegishi, PhD, Kiyoshi Sato, MD, PhD, Takashi Togo, MD, PhD, Omi Katsuse, MD, PhD, Hirotake Uchikado, MD, PhD, Yoshiko Furukawa, MD, PhD, Hiroaki Hino, MD, PhD, Kenji Kosaka, MD, PhD, Piers C. Emson, PhD, Keiji Wada, MD, PhD, Valina L. Dawson, PhD, Ted M. Dawson, MD, PhD, Heii Arai, MD, PhD, and Eizo Iseki, MD, PhD

Abstract

Missense mutations in the *leucine-rich repeat kinase 2* (*LRRK2*) gene are the most common causes of both familial and sporadic forms of Parkinson disease and are also associated with diverse pathological alterations. The mechanisms whereby *LRRK2* mutations cause these pathological phenotypes are unknown. We used immunohistochemistry with 3 distinct anti-LRRK2 antibodies to characterize the expression of LRRK2 in the brains of 21 subjects with various neurodegenerative disorders and 7 controls. The immunoreactivity of LRRK2 was localized in a subset of brainstem-type Lewy bodies (LBs) but not in cortical-type LBs, tau-positive inclusions, or TAR-DNA–binding protein-43–positive inclusions. The immunoreactivity of LRRK2 frequently appeared as enlarged granules or vacuoles within neurons of affected brain regions, including the substantia nigra, amygdala, and entorhinal cortex in patients with Parkinson disease or dementia with LBs. The volumes of LRRK2-positive granular structures in neurons of the entorhinal cortex were significantly increased in dementia with LBs brains compared with age-matched control brains ($p < 0.05$). Double immunolabeling demonstrated that these LRRK2-positive granular structures frequently colocalized with the late-endosomal marker Rab7B and occasionally with the lysosomal marker, the lysosomal-associated membrane protein 2. These results suggest that LRRK2 normally localizes to the endosomal-lysosomal compartment within morphologically altered neurons in neurodegenerative diseases, particularly in the brains of patients with LB diseases.

Key Words: Alzheimer disease, Dementia with Lewy bodies, Endosome, Leucine-rich repeat kinase 2, Lysosome, PARK8, Parkinson disease.

INTRODUCTION

Parkinson disease (PD), the second most common age-related neurodegenerative disorder after Alzheimer disease (AD), is characterized by neuronal degeneration with Lewy bodies (LBs) in the substantia nigra pars compacta that leads to dysfunction of the nigrostriatal dopaminergic pathway, striatal dopamine deficiency, and clinical parkinsonism. Although the etiology of PD is not known, genetic analysis has provided important new insights into its pathogenesis. Mutations in 6 genes are unambiguously associated with rare Mendelian forms of PD, including *α-synuclein* (1), *parkin* (2), *PTEN-induced putative kinase 1 (PINK1)* (3), *DJ-1* (4), *leucine-rich repeat kinase 2 (LRRK2)* (5, 6), and *ATP13A2* (7). Of these genes, missense mutations in *LRRK2* have been identified as the cause of late-onset autosomal-dominant parkinsonism linked to chromosome 12q11.2-q13.1 (PARK8 locus). A G2019S mutation in *LRRK2*, which is the most prevalent *LRRK2* variant, also accounts for apparently sporadic cases with PD (8). The disease penetrance in PD subjects with *LRRK2* mutations seems to be age dependent (9), and their clinical and neurochemical manifestations are not different from those of idiopathic PD subjects. More important, in some ethnic subgroups including North African Arabs, Ashkenazi Jews, and Arab-Berbers of Tunisia, there is a higher frequency of the G2019S variant in PD cohorts (10, 11). Therefore, the LRRK2 protein may provide important insights into the pathogenesis of PD. At present, however, the biologic and functional roles of the LRRK2 protein are not well characterized.

From the PET/CT Dementia Research Center, Juntendo Tokyo Koto Geriatric Medical Center, Juntendo University School of Medicine, Koto-ku (SH, RY, MM, KS, EI); Department of Degenerative Neurological Diseases, National Institute of Neuroscience, National Center of Neurology and Psychiatry, Kodaira-shi (SH, KW), Tokyo; Yokohama Houyuu Hospital, Asahi-ku, Yokohama (SH, HH, KK), Japan; Laboratory of Molecular Neurodegenerative Research, Brain Mind Institute, Ecole Polytechnique Fédérale de Lausanne, Lausanne, Switzerland (DJM); Department of Psychiatry, Juntendo University School of Medicine, Bunkyo-ku, Tokyo (RY, HA); Department of Psychiatry, Yokohama City University School of Medicine, Kanazawa-ku, Yokohama (TT, OK, HU, YF), Japan; Laboratory of Molecular Neuroscience, The Babraham Institute, Babraham, Cambridge, UK (PCE); Neuroregeneration and Stem Cell Programs, Institute for Cell Engineering (VLD, TMD), Departments of Neurology (VLD, TMD), Neuroscience (VLD, TMD), and Physiology (VLD), Johns Hopkins University School of Medicine, Baltimore, Maryland.

Send correspondence and reprint requests to: Shinji Higashi, MD, PhD, Department of Degenerative Neurological Diseases, National Institute of Neuroscience, National Center of Neurology and Psychiatry, 4-1-1 Ogawa-Higashi, Kodaira-shi, Tokyo 187-8502, Japan; E-mail: higashis@ncnp.go.jp

This research was supported by grants from the Kurata Memorial Hitachi Science and Technology Foundation (Shinji Higashi); Grants-in-Aid for Young Scientists (B), Grant No. 21790856 (Shinji Higashi), from the Japan Ministry of Education, Science, Sports and Culture (Eizo Iseko); Grant No. NS38377 (Ted M. Dawson) from the National Institutes of Health/National Institute of Neurological Disorders and Stroke; and by funding support from the Ecole Polytechnique Fédérale de Lausanne (Darren J. Moore).

In contrast to clinical manifestations that are consistent with idiopathic PD, the brains of patients with *LRRK2* mutations exhibit more diverse pathological alterations. In addition to the classical nigral degeneration predominantly with LB pathology found in the brains of patients with idiopathic PD and dementia with LBs (DLB) (8, 12–15), tau-positive inclusions reminiscent of tauopathies (15, 16), ubiquitin-positive pathology only (17), or the distinct absence of pathological inclusions (12, 18) are less commonly observed. These findings suggest that LRRK2 may be central to or upstream of pathogenic pathways that regulate α-synuclein or tau protein deposition and that disruptions of this pathway caused by *LRRK2* mutations precipitate a PD phenotype. To address this notion, several research groups have investigated the distribution of LRRK2 protein in normal and pathological human brains to determine whether it is localized to LBs or neurofibrillary tangles (NFTs) in synucleinopathies or tauopathies, respectively. The LRRK2 protein has been identified in various brain regions including the striatum, cerebral cortex, hippocampus, and cerebellum but at markedly lower levels in the substantia nigra (19–23). Nevertheless, LRRK2 protein is localized to a subset of α-synuclein–positive LBs in the substantia nigra pars compacta of PD and DLB brains (19, 24–27). Furthermore, a previous report showed that diverse tau-positive inclusions in the brains of patients with AD, parkinsonism dementia complex of Guam and Pick disease (PiD), and intraneuronal inclusions in the spinal cords of patients with amyotrophic lateral sclerosis were immunopositive for LRRK2, suggesting that it may also be localized to tau-positive inclusions in tauopathies and possibly ubiquitin-positive inclusions in TDP-43 proteinopathies (28). In contrast, others have reported that LRRK2 is not localized to NFTs (25). Thus, consistent results regarding the localization of LRRK2 protein in neurodegenerative disorders have not yet been obtained.

In the present study, we investigated a variety of neurodegenerative disorders and found that LRRK2 is localized to a subset of α-synuclein–positive brainstem-type LBs but not to α-synuclein–positive cortical-type LBs, tau-positive NFTs, or other tau inclusions, nor to TDP-43–positive inclusions. In addition, we often observed LRRK2-positive enlarged granules or vacuoles within neurons of the substantia nigra pars compacta and limbic area of pathological brains (particularly in PD and DLB brains) that are obviously distinct from the smaller LRRK2-positive punctate structures normally present in neurons of control brains. These pathological LRRK2-positive enlarged structures frequently colocalized with the late-endosomal marker, Rab7B, and occasionally with the lysosomal marker, lysosomal-associated membrane protein 2 (LAMP-2). These results suggest a role for LRRK2 in the endosomal-lysosomal system in the pathogenesis of LB diseases.

MATERIALS AND METHODS

Case Material

We examined 21 postmortem brains from patients with neurodegenerative disorders, including PD, DLB, AD, PiD, progressive supranuclear palsy, corticobasal degeneration, and frontotemporal lobar degeneration with ubiquitin inclusions (FTLD-U). The patients had no family history of neurological or psychiatric disorders. Clinical and demographic data are given in Table 1. The PD cases fulfilled the diagnostic criteria for PD (29), DLB cases fulfilled the consensus criteria for a high likelihood of DLB (30), and AD cases fulfilled consensus criteria for a high likelihood of AD (31). The neuropathologic features of each case of PD, DLB, and AD were assessed as previously described (32) (Table 2). In addition, 7 normal elderly control cases with no history of neurological disorders or no evidence of significant neuropathologic abnormalities were also studied (Table 1).

Antibodies

Rabbit polyclonal anti-LRRK2 antibodies were generated using keyhole limpet hemocyanin–coupled synthetic peptides corresponding to human LRRK2 amino acids 334 to 347 (JH5517) and 2500 to 2515 (JH5514), as previously described (35, 36). A commercial rabbit polyclonal anti-LRRK2 antibody, NB300-267, was also used (human LRRK2, amino acids 920–945, Novus Biologicals, Littleton, CO; [37]). These 3 anti-LRRK2 antibodies have previously been shown to recognize a protein band of approximately 280 kd, corresponding to the predicted size of LRRK2 protein by Western blot analysis of cell or tissue lysates and have been used in previous studies for immunohistochemistry (12, 19, 26–28, 35–38). Additional antibodies used were anti–phosphorylated α-synuclein (pSer129 [39]), anti-amyloid β, anti–paired helical filament (PHF) tau, anti-TAR-DNA–binding protein 43 (TDP-43), anti–LAMP-2, anti-Rab7B, anti–cytochrome oxidase *c* subunit IV (COX IV), and anti–trans-Golgi network protein 2 (TGOLN2 , also known as TGN38) (Table 3).

Immunohistochemical and Immunofluorescent Analysis

Cerebral hemispheres and brainstem, including the midbrain, pons and medulla oblongata, amygdala, hippocampus, entorhinal cortex, and inferior temporal cortex (Brodmann

TABLE 1. Clinical and Demographic Data

Group	n (Male-Female)	Age, Years	Brain Weight, g	Disease Duration, Years
PD	2 (1:1)	58 ± 19.8	1,190 ± 156	7 ± 1.4
DLB	6 (4:2)	69.3 ± 10.6	1,071 ± 137	4.8 ± 1.3
AD	6 (3:3)	77.3 ± 11	1,080 ± 124	7 ± 3.7
PiD	2 (1:1)	72.5 ± 2.1	790 ± 156	10.5 ± 6.4
PSP	1 (1:0)	67	1,160	5
CBD	1 (0:1)	72	867	16
FTLD-U	3 (2:1)	67.3 ± 3.1	1,008 ± 172	8.7 ± 3.8
Control	7 (4:3)	73.9 ± 5.2	1,294 ± 34	—

Ages, brain weights, and disease durations for each group are presented as mean ± SD.
Control, aged normal subjects.
AD, Alzheimer disease; CBD, corticobasal degeneration; DLB, dementia with Lewy bodies; FTLD-U, frontotemporal lobar degeneration with ubiquitin-positive inclusions; PD, Parkinson disease; PiD, Pick disease; PSP, progressive supranuclear palsy.

TABLE 2. Neuropathologic Data on Parkinson Disease, Dementia With Lewy Bodies, and Alzheimer Disease Cases

Case No.	Aβ Stage	NF Stage	Lewy Stage	AD Criteria	DLB Criteria
PD1	B	I	I>	NA	NA
PD2	A	I	I>	NA	NA
DLB1	C	IV	IV	NA	High (diffuse neocortical)
DLB2	C	II	III	NA	High (diffuse neocortical)
DLB3	0	II	IV	NA	High (diffuse neocortical)
DLB4	C	II	III	NA	High (diffuse neocortical)
DLB5	C	II	III	NA	High (diffuse neocortical)
DLB6	C	II	III	NA	High (diffuse neocortical)
AD1	C	V	NA	High	NA
AD2	C	V	NA	High	NA
AD3	C	IV	NA	High	NA
AD4	C	V	NA	High	NA
AD5	C	V	NA	High	NA
AD6	C	V	NA	High	NA

Amyloid β (Aβ) Stages (A–C) and neurofibrillary (NF) Stages (I–VI) were determined according to Braak staging (33). Lewy stages (I–IV) in dementia with Lewy bodies (DLB) were assigned according to our previous protocol (34). Consensus criteria were used to diagnose Parkinson disease (PD) (29), DLB (30), and AD (31).

NA, not applicable.

Area 20), of all brains were fixed in 4% paraformaldehyde in 0.1 mol/L phosphate buffer, pH 7.4 (PBS), embedded in paraffin, and cut into 6-μm-thick sections. After removal of the paraffin, endogenous peroxidase activity was quenched for 30 minutes with 1.5% H_2O_2 in methanol. After rehydration, antigens were retrieved with autoclaving or treatment with 70% formic acid. Sections were blocked for 1 hour with 10% normal goat or horse serum and then incubated overnight at 4°C with primary antibodies at the appropriate dilution (Table 3). Sections were incubated for 1 hour with biotinylated secondary antibody, either goat anti-rabbit or horse anti-mouse IgG (1:500, Vector Laboratories, Burlingame, CA), and processed for 45 minutes with avidin-biotin horseradish peroxidase complex (ABC) (Vector Laboratories). Immunoreactivity was visualized with 0.5 mg/mL 3,3,-diaminobenzidine tetrachloride and 0.03% H_2O_2. Washes (2 for 20 minutes each) in PBS were carried out between each step. The sections were lightly counterstained with hematoxylin, dehydrated through graded alcohols, cleared with xylene, and mounted in mounting medium. Some sections were also double immunostained with antibodies to LRRK2 and phosphorylated α-synuclein, PHF tau, LAMP-2, Rab7B, COX IV, or TGOLN2. Immunoreactivity was detected using the ABC–horseradish peroxidase and the ABC–alkaline phosphatase methods (ABC-alkaline phosphatase kit) (Vector Laboratories) and visualized with 3,3,-diaminobenzidine tetrachloride and fast blue, respectively. The sections were coverslipped with 90% glycerol in PBS.

For double labeling immunofluorescence, the primary antibodies were used at lower dilutions. After incubation overnight at 4°C in antibody to LRRK2 (JH5514, JH5517, or NB300-267; 1:200 dilution) together with antibody to PHF tau, LAMP-2, Rab7B, COX IV, or TGOLN2, the sections were incubated for 3 hours with AlexaFluor-488 goat anti-rabbit IgG for antibody to LRRK2 and AlexaFluor-594 goat anti-mouse IgG for antibody to PHF tau, LAMP-2, Rab7B, COX IV, or TGOLN2 (Molecular Probes, Carlsbad, CA). Immunofluorescence was visualized on an Olympus Fluoview FV1000 Confocal Microscope.

Morphometric Analysis

For the quantification of the LRRK2-immunoreactive area per cell in 6 DLB, 6 AD, and 7 aged control cases, immunohistochemistry was carried out under identical experimental conditions that resulted in comparable background staining intensities among all cases. For each brain, 25 neurons with the nucleolus in focus on the section were selected at random from several fields throughout the entorhinal cortex. Evaluation of LRRK2-immunoreactive areas for each neuron was performed with the Win Roof version 5 (Mitani Corp, Japan) at 1,000× magnification interfaced with an Olympus digital CCD camera (DP71) mounted on an Olympus BX51

TABLE 3. Antibodies

Antibody	Type, Species	Source and Reference	Staining Dilution
Anti-LRRK2 (JH5514)	Polyclonal, rabbit	In-house (Johns Hopkins)	1:400
Anti-LRRK2 (JH5517)	Polyclonal, rabbit	In-house (Johns Hopkins)	1:400
Anti-LRRK2 (NB300-267)	Polyclonal, rabbit	Novus Biologicals, Littleton, CO (37)	1:400
Anti–phosphorylated α-synuclein (Pser129)	Monoclonal, mouse	Gift from Dr. T. Iwatsubo, University of Tokyo, Tokyo, Japan (39)	1:20,000
Anti–amyloid-β	Polyclonal rabbit	Gift from Dr. T. Ishii (Sagamidai Hospital, Kanagawa, Japan)	1:5000
Anti–PHF tau (AT8)	Monoclonal, mouse	Innogenetics, Zwijnaarde, Belgium	1:2000
Anti–TDP-43 (10782-1-AP)	Polyclonal, rabbit	ProteinTech Group, Chicago, IL	1:2000
Anti–LAMP-2 (H4B4)	Monoclonal, mouse	Santa Cruz Biotechnology, Santa Cruz, CA	1:200
Anti-Rab7B (3B3)	Monoclonal, mouse	Abnova Corporation, Taipei, Taiwan	1:200
Anti–COX IV	Monoclonal, mouse	Abcam, Tokyo, Japan	1:400
Anti-TGN38/TGOLN2 (M02)	Monoclonal, mouse	Abnova Corporation, Taipei, Taiwan	1:200

COX IV, cytochrome oxidase *c* subunit IV; LAMP-2, lysosomal-associated membrane protein 2; PHF, paired helical filament; TDP-43, TAR-DNA binding protein 43; TGOLN2, trans-Golgi network protein 2.

microscope. The LRRK2-positive enlarged structures were selected as green immunoreactive dots using 2-color extraction in the Win Roof program. The areas were then measured. The total cytoplasmic area occupied by faint brown immunoreactivity was also selected as a green cytoplasmic area using 2-color extraction with similar threshold values in each section followed by the optical dissection of the nucleus if needed, and then the area was quantified. Differences in mean volume of LRRK2-positive enlarged structures among the 3 groups of brains were analyzed by 2-tailed unpaired Student *t*-test; values of $p < 0.05$ were considered significant. Measurements of the diameter of LRRK2-positive enlarged structures in the digital images were carried out using the measurement program of line length of the Win Roof software.

Cell Counting

The numbers of neurons with or without enlarged structures, in which LRRK2 immunoreactivity colocalized to Rab7B immunoreactivity, were counted using microscopic fields at 400× magnification (field size, 0.025 mm^2) in the basal amygdaloid nucleus of DLB brains. The average numbers of neurons in 3 fields were calculated in each DLB case for determining the proportions of neurons with double-positive enlarged structures.

RESULTS

LRRK2 Localizes to Brainstem-Type LBs but Not to Tau- or TDP-43–Positive Pathological Inclusions

We previously reported that a small subset of brainstem-type LBs in the substantia nigra pars compacta in 2 PD cases were immunoreactive for LRRK2 using 2 distinct anti-LRRK2 antibodies (19). Here, we investigated the localization of LRRK2 in the brainstem of 2 PD and 6 DLB cases using 3 anti-LRRK2 antibodies that were raised against distinct LRRK2 peptide sequences (Fig. 1A). LRRK2 immunoreactivity was observed in a small subset of brainstem-type LBs in the substantia nigra pars compacta, locus coeruleus and dorsal vagal nucleus of PD and DLB brains (Figs. 1B–G). The immunoreactivity was predominantly localized to the core (Figs. 1B, D, E, G) or to the rim surrounding the core (Figs. 1C, F) of the LBs; the LB halos were usually LRRK2-immunonegative. The LRRK2 immunopositivity in these LBs colocalized with phosphorylated α-synuclein (Figs. 1H, I), although the latter was predominant in the halos. Counts in consecutive sections immunostained with 1 of these antibodies indicated that approximately 15% to 40% of phosphorylated α-synuclein-positive brainstem-type LBs are also immunopositive for LRRK2.

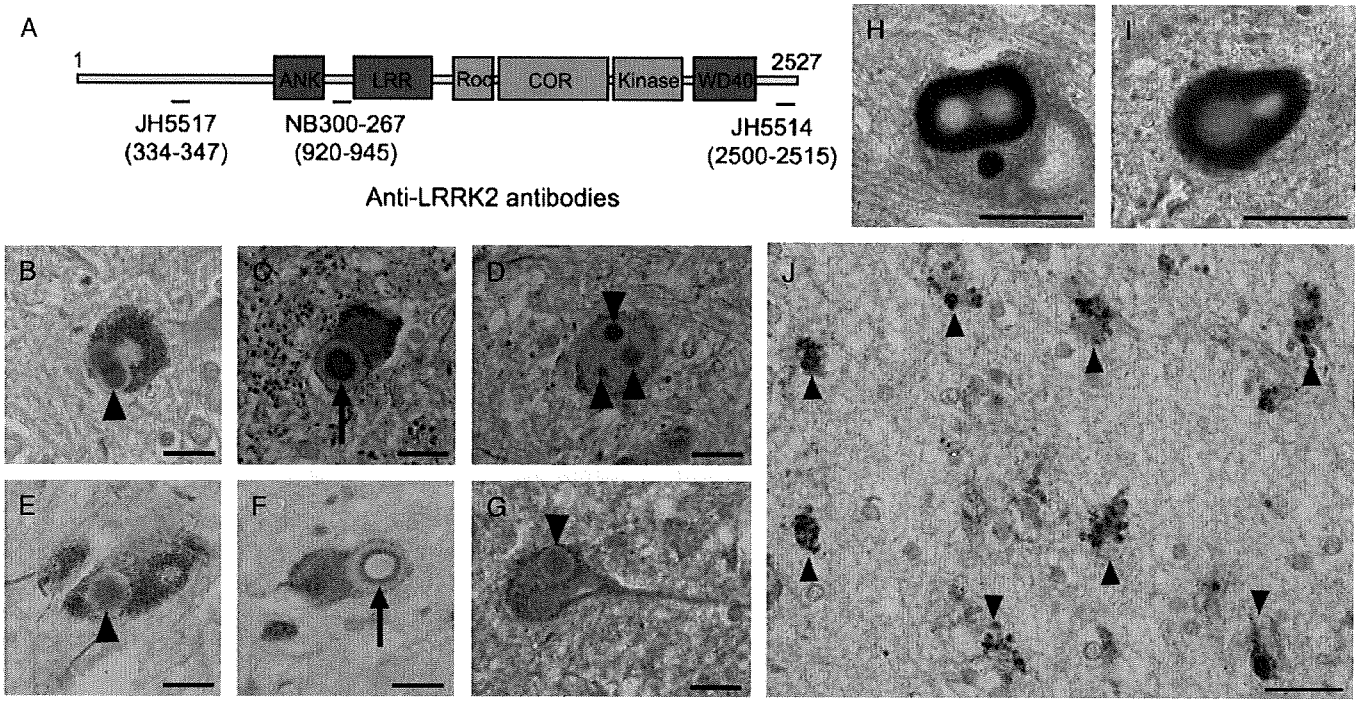

FIGURE 1. Localization of leucine-rich repeat kinase 2 (LRRK2) in the brains of Parkinson disease (PD) and dementia with Lewy bodies (DLB) cases. **(A)** The location of peptides recognized by 3 LRRK2-specific polyclonal antibodies are shown aligned to the protein domain structure of LRRK2. **(B–G)** The immunoreactivity of LRRK2 in the core (arrowheads) and its outer rim (arrows) of brainstem-type LBs in the substantia nigra pars compacta **(B, E)**, locus caeruleus **(C, D, G)**, or dorsal vagal nucleus **(F)** of PD **(B, C, E, F)** or DLB **(D, G)** brains. **(H, I)** Double immunolabeling for LRRK2 (brown) and phosphorylated α-synuclein (blue) shows colocalization of LRRK2 with α-synuclein–positive brainstem-type LBs (dark brown). **(J)** The immunohistochemistry of LRRK2 in the amygdala of a DLB brain; LRRK2-positive enlarged granules are observed within the cytoplasm of neurons (arrowheads). Scale bar = 20 μm.